An Energy Efficient Cooperative Spectrum Sensing for Cognitive Radio-Internet of Things with Interference Constraints

Md Sipon Miah (m.miah1@nuigalway.ie)
Islamic University https://orcid.org/0000-0002-6986-1517
Mohammad Amzad Hossain
National University of Ireland Galway
Kazi Mowdud Ahmed
Islamic University
Md. Mahbubur Rahman
Islamic University
Ali Calhan
Duzce University: Duzce Universitesi

Research Article

Keywords: Cognitive radio, Energy detection, Internet of things, Spectrum sensing, Sum rate, Spectral efficiency, Expected life time, Energy consumption efficiency, Global error probability

Posted Date: February 10th, 2021

DOI: https://doi.org/10.21203/rs.3.rs-217608/v1

Wireless Personal Communications manuscript No.
(will be inserted by the editor)

An Energy Efficient Cooperative Spectrum Sensing for Cognitive Radio-Internet of Things with Interference Constraints

Md Sipon Miah [1] · Mohammad Amzad Hossain [2,3] · Kazi Mowdud Ahmed[1] · Md. Mahbubur Rahman[1] · Ali Calhan[4]

Received: date / Accepted: date

Abstract Spectrum sensing plays a very important role in Cognitive Radio based Internet of Things (CR-IoT) networks for utilization of the licensed spectrum accurately. However, the performance of the conventional Energy Detector (ED) method is compromised in a noise-uncertain environment owing to interference constraints, i.e. the CR-IoT user interference with the licensed Primary User (PU) on the same licensed band. To overcome this drawback, we proposed an energy efficient Cooperative Spectrum Sensing (CSS) for a CR-IoT network with interference constraints using a novel ED method. In this method, each CR-IoT user is capable of spectrum sensing that makes both the local decision and the weight factor based on the sequential approach; we calculate the weight factor against each CR-IoT user based on the Kullback Leibler Divergence award score. After the local decision and the weight factor are made, each CR-IoT user transmits its measured both the local decisions, and the weight factor to a Fusion Center (FC), which is made a final decision about the PU activities based on the hard fusion rule. The simulation results demonstrates that the proposed ED method obtains an improved detection performance, an enhanced sum rate, a spectral efficiency, an energy efficiency,

Md Sipon Miah
E-mail: sipon@ict.iu.ac.bd
· Mohammad Amzad Hossain
E-mail: m.hossain3@nuigalway.ie
· Kazi Mowdud Ahmed
E-mail: mowdud@ice.iu.ac.bd
· Md. Mahbubur Rahman
E-mail: drmahbub_07@yahoo.com
· Ali Calhan
E-mail: alicalhan@duzce.edu.tr
[1] Dept. of Information and Communication Technology, Islamic University, Kushtia-7003, Bangladesh
[2] School of Computer Science, National University of Ireland Galway, Ireland
[3] Dept. of Information and Communication Engineering, Noakhali Science and Technology University, Noakhali, Bangladesh
[4] Department of Computer Engineering, Duzce University, Duzce, Turkey

and a lower global error probability when compared to other conventional ED methods under time varying environments.

Keywords Cognitive radio · Energy detection · Internet of things · Spectrum sensing · Sum rate · Spectral efficiency · Expected life time · Energy consumption efficiency · Global error probability

1 Introduction

Nowadays the Internet of Things (IoT) is one of the most rising network applications that connects the billions of networking devices across the globe to the Internet world and permits connectivity among devices, all networking appliances can collect and share data continuously over the internet to achieve better value and services [1–6]. Nevertheless, there are several challenges that abate the outgrowth of IoT networks such as its requires greater bandwidth for connecting a lot number of hybrid communication devices and services, ensuring the security of a massive number of heterogeneous devices and networks, high implementation cost, lack of adequate spectrum and more energy required than the conventional communication systems [7–11]. Cognitive Radio (CR) technology is developed to solve the spectrum shortage due to increasing wireless devices and networks [12–14]. It promotes the use of the radio frequency band by permitting Secondary User (SU) to allow the licensed spectrum of the Primary User (PU) [15–20]. In a Cognitive Radio based IoT (CR-IoT) network [4, 21, 22], each CR-IoT user is conveniently using the idle licensed frequency bandwidth when the licensed user is absent in the CR-IoT networks. Basically, each CR-IoT user detects the unoccupied licensed channels and selects the one that is most appropriate for data transmission. To overcome the unacceptable conflict between the PU and the CR-IoT user, the CR-IoT user leaves the licensed spectrum as soon as possible when the PU returns to transmit data in the network [23, 24]. The unoccupied licensed spectrum detection is a very important part in the CR Network (CRN) to overcome the unacceptable conflict between the PU and the SU [25, 26].

Licensed spectrum detection approaches can be classified into many groups, including non-coherent spectrum sensing, coherent spectrum sensing, Non-Cooperative Spectrum Sensing (NCSS), and Cooperative Spectrum Sensing (CSS). In a non-coherent spectrum sensing, for the purpose of spectrum sensing it is not require any previous knowledge about the PU signal [27]. In a coherent detection scheme, PU signal detection requires perfect prior knowledge of the PU signal, e.g. synchronization message, presenter, spectral scattering sequences, training and pilot patterns [28]. In non-cooperative detection, CR-IoT users do not need to exchange sensing information with other CR-IoT users [29]. In this method, the performance of spectrum detection is reduced due to concealed terminal issues, multi-path fading, and shadow impact [30]. In CSS techniques [31, 32], where group of CR-IoT users cooperatively execute spectrum detection to mitigate the multi-path fading, hidden terminal problem, and shadowing effects. In CSS technique, each CR-IoT user sends

the spectral detection result of the PU signal to the respective Fusion Center (FC) individually. Thereafter, the FC uses the fusion rule on the collected spectrum detection outcomes of the CR-IoT users to take a final global decision. In the end, the FC transfers a final global decision to all CR-IoT user about the appearance and non-appearance of the PU signal in the CR-IoT networks [33–35].

Numerous spectrum sensing methods have been investigated under varying conditions, including matched filter method [36], cyclostationary feature method [37], entropy-based method [39,40], eigenvalue-based method [38], and Energy Detection (ED) method [41,42]. The matched filter method and cyclostationary feature method are both easy to understand and execute. However, both require reliant prior knowledge of PU signals, e.g., the carrier frequency, the modulation technique, amplitude, and phase of the PU signal [43]. The ED method is one of the simplest methods to calculate the received signal energy of the PU signal without any previous information about the PU signal [44]. Therefore, it is the most commonly used method for spectrum sensing in CRNs. However, the ED is very susceptible to noise fluctuations and needs a absolutely right understanding of the influence of noise signal power at the receiver side of the CR-IoT user for proper identification of PU signal. As a result, the detection performance of the ED method is degraded in noise uncertainty environments and low Signal to Noise Ratio (SNR) value [45].

The CSS technique was studied in order to resolve the issue of spectrum sensing for CR-IoT networks. In [46], the detection performance of CSS have been analyzed under a situation in which malicious users transfer a wrong detection result to the FC, i.e. malware attacks. In [47], the authors introduced the eigenvalue-based CSS scheme to enhance the spectrum detection performance under the effects of impulsive noise distributions. In [48], the authors analysed the blind CSS methods for interweave CRN. In [49] each CR-IoT user used the CSS technique to sense the PU signal, they are used noisy reporting channel to send the sensing results to the FC. In [50], the authors used the Kullback-Leibler divergence (KLD) technique to calculate the weight value for each CR-IoT user according to their local sensing result and the FC uses the local sensing results and weight value of each CR-IoT user to make the final global decision about the appearance and non-appearance of the PU's signal in CR-IoT networks. In [51], each CR-IoT generates their local spectrum sensing result about the appearance and non-appearance of the PU's signal in the network. The FC collected the local detection results. Thereafter, the FC applies weights to the local spectrum detection results of the CR-IoT users. Finally, the FC makes the final global decision based on the KLD techniques and this decision sends to the CR-IoT users. The authors proposed sub-optimal recursive search algorithm to maximize energy efficient licensed spectrum detection for a CRN by optimizing sensing and transmission time in [52]. Its minimizes the interference between PU and cognitive user transmission. However, their paper considered only one PU and one SU; for the large number of SUs, this scheme is not capable of ensuring optimal spectrum detection performance. In [53], the authors proposed the Conventional Col-

Table 1: Comparison of existing ED methods to proposed ED method for scenario $\mathbb{I}$ and scenario $\mathbb{III}$ in a CR-IoT network

Approaches	Proposed idea	ED	$\mathbb{I}/\mathbb{III}$	$p_{d,FC}$	$\mathbb{R}$	$\mathbb{V}_{SE}$	$\mathbb{V}_{EE}$	p_e
M. S. Miah et al. (2020) [5]	Enhanced Sensing and Sum-Rate Analysis in a CR-IoT	✓	$\mathbb{I}$	✓	✓	✗	✗	✗
I. Develi (2020) [60]	Spectrum sensing in CRNs: threshold optimization and analysis	✓	$\mathbb{I}$	✓	✗	✗	✗	✓
Z. Tabakovic et al. (2016) [61]	Cognitive radio frequency assignment with interference weighting and categorization	✓	$\mathbb{III}$	✓	✓	✗	✗	✗
S. Biswas et al. (2019) [62]	Sum throughput maximization in a cognitive multiple access channel with CSS and energy harvesting	✓	$\mathbb{I}/\mathbb{III}$	✓	✓	✗	✗	✗
X. Liu, et al. (2020) [63]	CSS optimization in energy-harvesting for CRNs	✓	$\mathbb{I}$	✓	✓	✗	✗	✗
M. S. Miah et al. (2021) [64]	Machine learning-based malicious user detection in energy harvested CR-IoT	✓	$\mathbb{I}$	✓	✓	✗	✓	✗
M. S. Miah et al. (proposed)	An energy efficient cooperative spectrum sensing for CR-IoT with interference constraints	✓	$\mathbb{I}/\mathbb{III}$	✓	✓	✓	✓	✓

laborative Compressive Sensing (CCCS) approach for better energy efficiency spectrum sensing in CRNs. Their paper optimized the parameters value to enhance the energy efficiency of the CCCS scheme. The authors introduced the energy efficient spectrum sensing approach using Dempster–Shafer (D-S) theory in CR Sensor Networks (CRSNs) to maximize detection accuracy and minimize energy consumption in [54]. In [55], the authors proposed a two-way dynamic spectrum sensing scheme which the energy efficiency for data transmission in CR-IoT networks are maximized. Moreover, the proposed an energy efficient power assignment approach is to improve the spectrum detection performance and throughput. In [56], the authors proposed a hybrid PSO (Particle Swarm Optimization)-GSA (Gravitational Search Algorithm) which is maximized the energy efficiency of the spectrum detection by identifying the licensed spectrum, the power spectral density and the transmission power.

In summary, the current research has some drawbacks as shown in Table 1: (i) a typical CR-IoT network in which all CR-IoT users are participating to sense the PU licensed channel for scenario $\mathbb{I}$ which did not to consider interference constraints e.g., perfect channel conditions; and (ii) an improved detection performance, an enhanced the sum rate, an improved spectral efficiency, a lowest energy efficiency and a lowest global error probability for scenario $\mathbb{III}$ has not been analyzed regarding with both interference constraints e.g., imperfect channel conditions and flexible sensing time e.g., sequential scheduling. The proposed ED method overcomes these drawbacks.

The major achievements of this article are summarized in the following points:

- We propose an energy efficient CSS scheme for CR-IoT networks with interference constraints $\mathbb{III}$. The sum rate in the proposed scheme using a novel ED method is an analyzed and an evaluated. The feasibility of the proposed ED method is evaluated when compared with the conventional ED method for scenario $\mathbb{I}$, e.g., detection performance and sum rate.
- We examine the sequential approach [2] in which the flexible sensing time period is obtained by each CR-IoT user, which enhances the detection performance, however with the limited number of samples due to noise uncertainty [27] and interference robustness. In addition, we evaluate the weight factor from the KLD award score based on the flexible sensing time slot.
- The detection performance of the proposed ED method is analyzed for both CR-IoT users and an FC based on the hard fusion rule.
- Depending on the enhanced detection performance, (i) the sum rate of the licensed primary network, and the unlicensed CR-IoT network, is evaluated for the conventional ED method and the proposed ED method using the hard fusion rule under different channel environments, and (ii) the global error probability is also evaluated for the conventional ED method and the proposed ED method with interference constraint for scenario $\mathbb{III}$.
- Moreover, the spectral efficiency and the energy efficiency are analyzed depend on both the sum rate and the detection performance for the conventional ED method and the proposed ED method with interference constraint for scenario $\mathbb{III}$.
- Eventually, the simulation results show that the proposed ED method obtains an improved detection performance, an enhanced sum rate, an improved spectral efficiency, a lowest energy efficiency and a lowest global error probability compared to other conventional ED methods with interference constraints for scenario $\mathbb{III}$.

The rest of this article is structured as follows. The proposed system model for scenario $\mathbb{I}$ and scenario $\mathbb{III}$ explains in Section 2. The conventional ED method for scenario $\mathbb{I}$ is discussed in Section 3. Moreover, we describe the detection performance, the sum rate, the spectral efficiency, an energy efficiency, and the global error probability. In Section 4, the proposed scheme based on a novel ED method for scenario $\mathbb{III}$ is analyzed of the flexible sensing duration, the weight factor based on the KLD award score, the detection performance, the sum rate, the spectral efficiency, an energy efficiency, and the global error probability. The simulation validation with the value of parameters and their affects are discussed in Section 5, here, the proposed ED method illustrates improved detection performance, enhanced sum rate, spectral efficiency, energy efficiency, global error probability, and total time when compared to other conventional ED methods. Finally, in Section 6, our finding and possible future work are discussed.

For ease of comparison, in Table 2, we list our generally used notations with description as follows:

Table 2: **List of notations**

Notation	Description
H_0	Hypothesis representing the PU's signal present
H_1	Hypothesis representing the PU's signal absent
$\mathbb{M}$	Total number of the CR-IoT users
N_s	Total number of samples during sensing phase
f_s	Sampling frequency
τ_r	Duration of the fixed reporting time slot
$\mathbb{T}$	Duration of a total frame
γ	Signal to Noise Ratio (SNR) for scenario $\mathbb{I}$
τ_s^c/τ_s^p	Duration of a rigid sensing time slot/ a flexible sensing time slot
$\overline{\gamma}$	Signal to Interference plus Noise Ratio (SINR) for scenario $\mathbb{III}$
$x(l)$	Signal transmitted by the PU at symbol time l
$y_i(l)$	Noise of the i^{th} CR-IoT user at symbol time l
$z_i\,(l)$	Received signal by the i^{th} CR-IoT user at symbol time l
$h_i\,(l)$	Channel gain at symbol time l
SNR_{PU}	SNR of the PUs link
$SNR_{CR-IoT,i}$	SNR of the secondary link between the i^{th} CR-IoT user and the corresponding receiver
$p^{\mathbb{I}}_{f,i}/p^{\mathbb{III}}_{f,i}$	Probability of false alarm of the i^{th} CR-IoT user for scenarios $\mathbb{I}$/ $\mathbb{III}$
$p^{\mathbb{I}}_{d,i}/p^{\mathbb{III}}_{d,i}$	Detection probability of the i^{th} CR-IoT user for scenarios $\mathbb{I}/\mathbb{III}$
$\lambda^{\mathbb{I}}_{i,ED}/\lambda^{\mathbb{III}}_{i,ED}$	Local decision threshold for i^{th} CR-IoT user with an ED method for scenarios $\mathbb{I}/\mathbb{III}$
$p^{\mathbb{I}}_{f,FC}/p^{\mathbb{III}}_{f,FC}$	Global probability of false alarm at the FC for scenarios $\mathbb{I}/\mathbb{III}$
ω_i	Weight factor of the i^{th} CR-IoT user
$p^{\mathbb{I}}_{d,FC}/p^{\mathbb{III}}_{d,FC}$	Global detection probability at the FC for scenarios $\mathbb{I}/\mathbb{III}$
$\beta^{\mathbb{I}}/\beta^{\mathbb{III}}$	Global decision threshold at the FC for scenarios $\mathbb{I}/\mathbb{III}$
α	Primary activity factor
$\mathbb{R}^{\mathbb{I}}/\mathbb{R}^{\mathbb{III}}$	Sum rate at the FC for scenarios $\mathbb{I}/\mathbb{III}$
$\mathbb{V}^{\mathbb{I}}_{SE}/\mathbb{V}^{\mathbb{III}}_{SE}$	Spectral efficiency at the FC for scenarios $\mathbb{I}/\mathbb{III}$
$\mathbb{V}^{\mathbb{I}}_{EE}/\mathbb{V}^{\mathbb{III}}_{EE}$	Energy efficiency at the FC for scenarios $\mathbb{I}/\mathbb{III}$
$p^{\mathbb{I}}_e/p_e\mathbb{III}$	Global error probability at the FC for scenarios $\mathbb{I}/\mathbb{III}$

2 System Model

For a CR-IoT network, spectrum sensing become an essential and fundamental method to identify the unused spectrum allotted to the PUs. An explanation of the proposed system model for scenario $\mathbb{I}$, and scenario $\mathbb{III}$ are discussed in this section.

2.1 Scenario $\mathbb{I}$

The proposed system model is composed of a CR-IoT network (unlicensed), and a primary network (i.e., licensed) which is depicted in Fig. 1. The primary network is composed of the primary receiver (i.e., PU $\mathbb{R}$x), and the primary transmitter (i.e., PU $\mathbb{T}$x). The execution of the PU activities i.e., ON or OFF

are represented by the Time Division Multiplexing Access (TDMA). Whilst, in a CR-IoT network (i.e., secondary network), it includes an FC and a lot of ($\mathbb{M}$) CR-IoT users (unlicensed). Just in Fig. 1 (a) for scenario $\mathbb{I}$, the CR-IoT user refers to an unlicensed CR-IoT user who wants to access the PU spectrum without interference constraints from the casing, whereas the PU is referred to as the spectrum's licensed user.

2.2 Scenario $\mathbb{III}$

In this Fig. 1 (b) for scenario $\mathbb{III}$, the CR-IoT user refers to an unlicensed CR-IoT user who wants to allow the PU spectrum opportunistically with casing interference. As a result, this interference is degraded the detection performance of the proposed ED method.

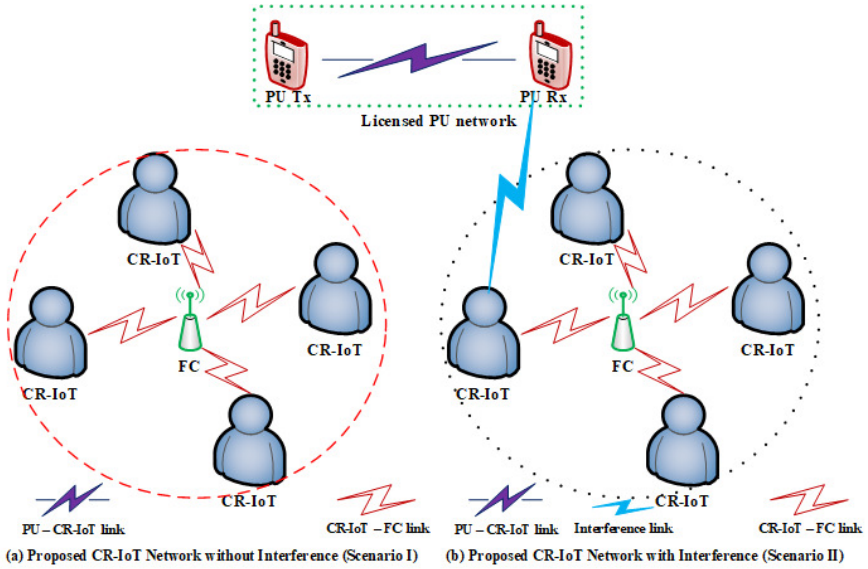

Fig. 1: The proposed system model for (a) Scenario $\mathbb{I}$ means without interference constraints, and (b) Scenario $\mathbb{III}$ means with interference constraints

Now, we define the hypotheses ($\mathbb{H}_1/\mathbb{H}_0$) describing the presence and absence of the PUs signal using a binary hypothesis testing problem as the following below:

$$\begin{cases} \mathbb{H}_0: & \text{the absence of the PUs signal on the channel,} \\ \mathbb{H}_1: & \text{the presence of the PUs signal on the channel.} \end{cases} \tag{1}$$

As a result, depend on the transmission of the PU activities, the received signal is evaluated by the i^{th} CR-IoT user under hypotheses as follows [57]:

$$z_i(l) = \begin{cases} x_i(l); & \mathbb{H}_0 \\ h_i(l)\, s(l) + x_i(l); & \mathbb{H}_1 \end{cases} \tag{2}$$

where $z_i(l)$ indicates the received signal in the l^{th} sampling time by the i^{th} CR-IoT user, $h_i(l)$ indicates the channel gain between the PU $\mathbb{T}$x and the i^{th} CR-IoT $\mathbb{R}$x, $x_i(l)$ indicates an additive white Gaussian noise of the i^{th} CR-IoT user, i.e., $x_i(l) \simeq \left(0, \sigma^2_{x,i}\right)$, and $s(l)$ indicates the transmitted PU signal that is used the Binary Phase Shift Keying (BPSK) modulation technique; here $l = 1, 2, \cdots, N_x$, and $i = 1, 2, \cdots, \mathbb{M}$. Moreover, during the sensing phase, the stationary channel is considered.

3 Conventional Energy Detection Method for Scenario $\mathbb{I}$

For the conventional ED method based CSS in CR-IoT networks for scenario $\mathbb{I}$ where the analysis of detection performance is addressed in the sub-section 3.1, the analysis of sum rate is provided in sub-section 3.2, the spectral efficiency is discussed in the sub-section 3.1, and the energy efficiency is discussed in sub-section 3.4. Moreover, the global error probability is discussed in the sub-section 3.5.

The received signal energy during the sensing phase of the conventional ED method is evaluated and compared with the predetermined threshold value [17, 18], which is illustrated in Fig. 2.

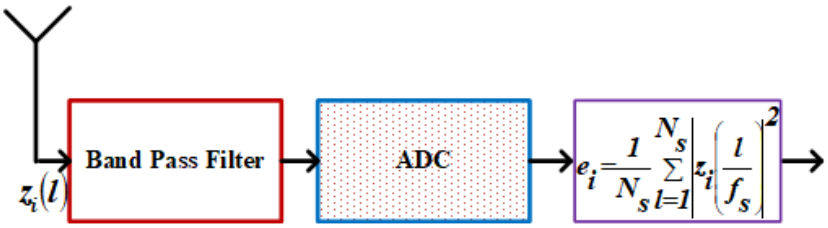

Fig. 2: The schematic description of the conventional ED method [17]

Now, the continuous signal power in time-domain that occupies the specific bandwidth is calculated by each CR-IoT user to achieve the decision statistics of the conventional ED method as described in the following: First, to choose the specified signal frequency, the obtained signal is filtered by a bandpass filter, and the outcome of that filter is converted by an analog to digital converter (ADC) as a produce the analog signal; Secondly, this analog signal is to produce the discrete time signal using sample and hold circuit; and Finally, this discrete time signal is independently summation and squared to calculate

its own signal energy obtained by the conventional ED method [58]. Therefore, the calculated energy of the i^{th} CR-IoT user is given by the following formula:

$$e_i = \sum_{l=1}^{N_s} \left\| z_i \left(\frac{l}{f_s} \right) \right\|^2 \tag{3}$$

where $z_i \left(\frac{l}{f_s} \right)$ is the received signal at the l^{th} sample of the i^{th} CR-IoT user, N_s indicates the signal samples during the sensing phase that defines as $N_s = 2\tau_s f_s$; here, f_s indicates the sampling frequency, and τ_s indicates the sensing time slot during the sensing phase. For all CR-IoT users in CR-IoT networks, thus, the duration of the inflexible sensing time slot, τ_s, is widely to use as shown in Fig. 3.

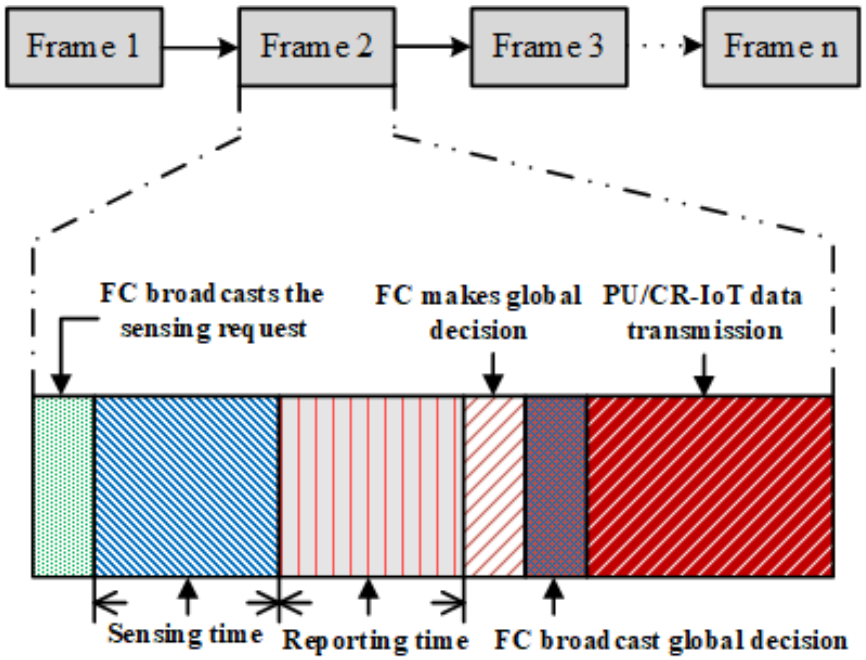

Fig. 3: Packet (i.e., each packet consists of the number of frames) format of the typical ED method for scenario $\mathbb{I}$ [2, 5, 17]

3.1 Analysis of detection Performance

If $N_s > 300$, then the measured obtained signal of the CR-IoT user, e_i, should be Gaussian random variable under both hypotheses based on the Center Limit

Theorem (CLT) that is mathematically defined as follows:

$$e_i \sim \begin{cases} \aleph\left(\mu_i\left(\mathbb{H}_0\right), \sigma_i^2\left(\mathbb{H}_0\right)\right) \\ \aleph\left(\mu_i\left(\mathbb{H}_1\right), \sigma_i^2\left(\mathbb{H}_1\right)\right) \end{cases} \tag{4}$$

where

$$\begin{aligned} \mu_i\left(\mathbb{H}_0\right) &= 2\tau_s^c f_s \sigma_{z,i}^2, \\ \sigma_i^2(\mathbb{H}_0) &= 2\tau_s^c f_s \sigma_{z,i}^4, \\ \mu_i\left(\mathbb{H}_1\right) &= 4\tau_s^c f_s \left(1+|h_i|^2\gamma_i\right)\sigma_{z,i}^2, \\ \sigma_i^2(\mathbb{H}_1) &= 4\tau_s^c f_s \left(1+2|h_i|^2\gamma_i\right)\sigma_{z,i}^4, \end{aligned}$$

where τ_s^c denotes the inflexible sensing time slot for the conventional ED method, and γ_i denotes SNR of the i^{th} CR-IoT user that is mathematically defined as $\gamma_i = \frac{p_s^2}{\sigma_{x,i}^2}$; here p_s denotes the signal power of the PU transmitted signal.

By comparing e_i to a predetermined threshold value, $\lambda_{i,ED}^{\mathbb{I}}$ using the Eq. 4, the detection probability, $p_{d,i}^{\mathbb{I}}$, and the probability of false alarm, $p_{f,i}^{\mathbb{I}}$ of the i^{th} CR-IoT user is calculated as follows:

$$\begin{aligned} p_{d,i}^{\mathbb{I}} =& Pr\left[e_i \geq \lambda_{i,ED}^{\mathbb{I}} | \mathbb{H}_1\right] \\ =& \mathbb{Q}\left(\frac{\lambda_{i,ED}^{\mathbb{I}} - \mu_i\left(\mathbb{H}_1\right)}{\sigma_i^2(\mathbb{H}_1)}\right) \\ =& \mathbb{Q}\left(\frac{\lambda_{i,ED}^{\mathbb{I}}}{\sqrt{2\tau_s^c f_s(1+2|h_i|^2\gamma_i)}\sigma_{z,i}^2} - \frac{\sqrt{2\tau_s^c f_s}(1+|h_i|^2\gamma_i)}{\sqrt{(1+2|h_i|^2\gamma_i)}}\right), \end{aligned} \tag{5}$$

and

$$\begin{aligned} p_{f,i}^{\mathbb{I}} = Pr\left[e_i \geq \lambda_{i,ED}^{\mathbb{I}} | \mathbb{H}_0\right] =& \mathbb{Q}\left(\frac{\lambda_{i,ED}^{\mathbb{I}} - \mu_i\left(\mathbb{H}_0\right)}{\sigma_i^2\left(\mathbb{H}_0\right)}\right) \\ =& \mathbb{Q}\left(\frac{\lambda_{i,ED}^{\mathbb{I}}}{\sqrt{2\tau_s^c f_s}\sigma_{z,i}^2} - \sqrt{2\tau_s^c f_s}\right) \end{aligned} \tag{6}$$

where $\mathbb{Q}\left(\theta\right)$ is a Gaussian tail function which is mathematically given by $\mathbb{Q}\left(\theta\right) = \frac{1}{\sqrt{2\pi}} \int_\theta^\infty e^{-\frac{\eta^2}{2}} d\eta$.

Therefore, the probability of a false alarm, $p_{f,i}^{\mathbb{I}}$ refers to the probability where the CR-IoT user wrongly claims the presence of the PU, even if the PU is really absent on the licensed spectrum for scenario $\mathbb{I}$; whilst the detection probability, $p_{d,i}^{\mathbb{I}}$ refers to the probability where the CR-IoT user correctly claims the presence of the PU, even though the PU is really present on the licensed spectrum for scenario $\mathbb{I}$.

After the sensing phase, each CR-IoT user forwarded its own local decision toward the respective FC during the fixed reporting time slot, which are

integrated with the local decisions in terms of achieving the global decision on the spectrum allocation of the PU [57]. Now, the detection performance of the global decision, i.e., $\left(p^{\mathbb{I}}_{f,FC}/p^{\mathbb{I}}_{d,FC}\right)$, at the FC for scenario $\mathbb{I}$ is calculated by

$$p^{\mathbb{I}}_{f,FC} = \begin{cases} 1, & if \sum_{i=1}^{\mathbb{M}} p_{f,i} < \beta^{\mathbb{I}} \\ 0, & otherwise \end{cases} \tag{7}$$

and

$$p^{\mathbb{I}}_{d,FC} = \begin{cases} 1, & if \sum_{i=1}^{\mathbb{M}} p_{d,i} \geq \beta^{\mathbb{I}} \\ 0, & otherwise \end{cases} \tag{8}$$

where $\beta^{\mathbb{I}}$ is the predetermined decision threshold at the FC for scenario $\mathbb{I}$.

3.2 Analysis of Sum Rate

The sum rate, $\mathbb{R}^{\mathbb{I}}$ of the conventional ED method for scenario $\mathbb{I}$, can be estimated based on the global detection performance $(p^{\mathbb{I}}_{f,FC}/p^{\mathbb{I}}_{d,FC})$ as follows:

$$\mathbb{R}^{\mathbb{I}} = \alpha p^{\mathbb{I}}_{d,FC} \mathbb{R}^{\mathbb{I}}_{PU} + (1-\alpha)\left(1 - p^{\mathbb{I}}_{f,FC}\right) \mathbb{R}^{\mathbb{I}}_{CR-IoT,i} \tag{9}$$

where α, $\mathbb{R}^{\mathbb{I}}_{PU}$, and $\mathbb{R}^{\mathbb{I}}_{CR-IoT,i}$ are the primary activity factor, the channel capacity of the PU link, and the channel capacity of the i^{th} CR-IoT user, respectively.

The channel capacity of the i^{th} CR-IoT user, and the channel capacity of the PU link are defined, respectively as follows:

$$\mathbb{R}^{\mathbb{I}}_{CR-IoT} = \frac{\mathbb{T} - \tau_s - \tau_r}{\mathbb{T}} \sum_{i=1}^{\mathbb{M}} \mathbb{W} \log_2 \left(1 + SNR_{CR-IoT,i}\right) \tag{10}$$

and

$$\mathbb{R}^{\mathbb{I}}_{PU} = \mathbb{W} \log_2 \left(1 + SNR_{PU}\right) \tag{11}$$

where $\mathbb{W}$ denotes the licensed channel bandwidth in bps/Hz.

3.3 Analysis of Spectral Efficiency

In this sub-section, the spectral efficiency (SE) of the conventional ED method without interference constraints for scenario $\mathbb{I}$ at the FC is evaluated which can be defined as follows:

$$\mathbb{V}^{\mathbb{I}}_{SE} = \frac{R^{\mathbb{I}}}{\mathbb{W}} \tag{12}$$

where $\mathbb{V}^{I}_{SE}$ is the SE for scenario $\mathbb{I}$ in b/s/Hz.

3.4 Analysis of Energy Efficiency

In this sub-section, the energy consumption (EE) of the conventional ED method without interference for scenario $\mathbb{I}$ at the FC is evaluated that is calculated as

$$\mathbb{V}_{EE}^{\mathbb{I}} = \frac{\mathbb{R}^{\mathbb{I}}}{\mathbb{P}} \tag{13}$$

where $\mathbb{V}_{EE}^{\mathbb{I}}$ is the EE of the conventional scheme without interference for scenario I in $b/s/\mathbb{J}$, and $\mathbb{P}$ is the transmitted power in $\mathbb{J}$.

3.5 Analysis of Global Error Probability

In this sub-section, the global error probability, $p_e^{\mathbb{I}}$ of the conventional ED method without interference for scenario $\mathbb{I}$ at the FC is evaluated which is formulated as follows:

$$p_e^{\mathbb{I}} = \alpha p_{f,FC}^{\mathbb{I}} + (1-\alpha)(1-p_{d,FC}^{\mathbb{I}}) \tag{14}$$

where α is the primary activity factor of the PU.

The whole idea is demonstrated by the Algorithm 1, which verifies the inflexible sensing time slot, $\tau_s^c = \tau_s$ (see line 3) as the conventional ED method without interference for scenario $\mathbb{I}$ is not being utilizing the reporting framework. After that, the probability of false alarm (see line 4), and the detection probability (see line 5) are determined in the conventional ED method without interference for scenario $\mathbb{I}$. Then after that, a global decision, $\left(p_{f,FC}^{\mathbb{I}}/p_{d,FC}^{\mathbb{I}}\right)$ at the FC is computed (see line 7/line 8). Finally, the sum rate, spectral efficiency, energy efficiency, and global error probability are computed based on the global detection $(p_{f,FC}^{\mathbb{I}}/p_{d,FC}^{\mathbb{I}})$ at the FC (see lines from 9 to 12).

4 Proposed Energy Detection Method for Scenario $\mathbb{III}$

For the proposed ED method based CSS with interference constraints in a CR-IoT network for scenario $\mathbb{III}$ where the utilization of the reporting framework is explained in the sub-section 4.1, the analysis of weight factor of each CR-IoT user is discussed in the sub-section 4.2, the analysis of detection performance is explained in the sub-section 4.3, the analysis of the sum rate is provided in sub-section 4.4, the spectral efficiency is derived in the sub-section 4.5, and finally, the energy efficiency is discussed in sub-section 4.6. Moreover, the global error probability is discussed in the sub-section 4.7 and the total time is discussed in sub-section 4.8.

Algorithm 1 The conventional ED method based CSS scheme without interference constraints for scenario $\mathbb{I}$

Input: $N_s, \mathbb{M}, \mathbb{T}, f_s, \tau_r$, **and** τ_s

Output: Estimate the probability of false alarm, $p^{\mathbb{I}}_{f,FC}$**, the detection probability,** $p^{\mathbb{I}}_{d,FC}$**, the sum rate** $\mathbb{R}^{\mathbb{I}}$**, the spectral efficiency,** $\mathbb{V}^{\mathbb{I}}_{SE}$**, the energy efficiency,** $\mathbb{V}^{\mathbb{I}}_{EE}$**, and the global error probability,** $p^{\mathbb{I}}_{e}$

1: Initialize $\mathbb{M}$, N_s, and τ_s
2: **for** $i = 1$ to $\mathbb{M}$ **do**
3: Calculate: $\tau^c_s = \tau_s$
4: Calculate: $p^{\mathbb{I}}_{f,i} = Pr[e_i \geq \lambda^{\mathbb{I}}_{i,ED} | \mathbb{H}_0]$
5: Calculate: $p^{\mathbb{I}}_{d,i} = Pr[e_i \geq \lambda^{\mathbb{I}}_{i,ED} | \mathbb{H}_1]$
6: **end for**
7: Calculate: $p^{\mathbb{I}}_{f,FC} = \begin{cases} 1; & if \sum_{i=1}^{\mathbb{M}} p^{\mathbb{I}}_{f,i} < \beta^{\mathbb{I}} \\ 0; & otherwise \end{cases}$
8: Calculate: $p^{\mathbb{I}}_{d,FC} = \begin{cases} 1; & if \sum_{i=1}^{\mathbb{M}} p^{\mathbb{I}}_{d,i} \geq \beta^{\mathbb{I}} \\ 0; & otherwise \end{cases}$
9: Calculate: $\mathbb{R}^{\mathbb{I}} = \alpha p^{\mathbb{I}}_{d,FC} \mathbb{R}^{\mathbb{I}}_{PU} + (1-\alpha)\left(1 - p^{\mathbb{I}}_{f,FC}\right) \mathbb{R}^{\mathbb{I}}_{CR-IoT,i}$
10: Calculate: $\mathbb{V}^{\mathbb{I}}_{SE} = \frac{\mathbb{R}^{\mathbb{I}}}{\mathbb{W}}$
11: Calculate: $\mathbb{V}^{\mathbb{I}}_{EE} = \frac{\mathbb{R}^{\mathbb{I}}}{\mathbb{P}}$
12: Calculate: $p^{\mathbb{I}}_{e} = \alpha p^{\mathbb{I}}_{f,FC} + (1-\alpha)(1 - p^{\mathbb{I}}_{d,FC})$

4.1 Analysis of Flexible Sensing Time

In flexible sensing time slot, the 2^{nd} CR-IoT user is utilized the fixed reporting time slot (τ^1_r) of the 1^{st} CR-IoT user as obtaining the flexible sensing time slot (τ^2_s), i.e., $\tau^2_s = \tau^2_s + \tau^1_r$; the 3^{rd} CR-IoT user is utilized the fixed reporting time slots of both the previous the 2^{nd} CR-IoT user (τ^2_r), and 1^{st} CR-IoT user (τ^1_r) as obtaining the more flexible sensing time slot (τ^3_s), i.e., $\tau^3_s = \tau^3_s + \tau^1_r + \tau^2_r$; etc as well, as depicted in Fig. 4. We conclude that the flexible sensing time slot (τ^p_s) is then obtained for all CR-IoT users, except for the 1^{st} CR-IoT user.

Currently, the flexible sensing time slot, τ^p_s, of the proposed ED method is calculated by each CR-IoT user in a CR-IoT network with interference constraints for scenario $\mathbb{III}$ which is seen in Fig. 4 of the following format [2]:

$$\tau^p_s = \tau_s + \sum_{i=1}^{\mathbb{M}-1} \tau^i_r \tag{15}$$

where τ_s, τ^p_s, and τ_r are the non-flexible sensing time slot for each CR-IoT user, the flexible sensing time slot of the proposed ED method, and the fixed reporting time slot for each CR-IoT user, respectively.

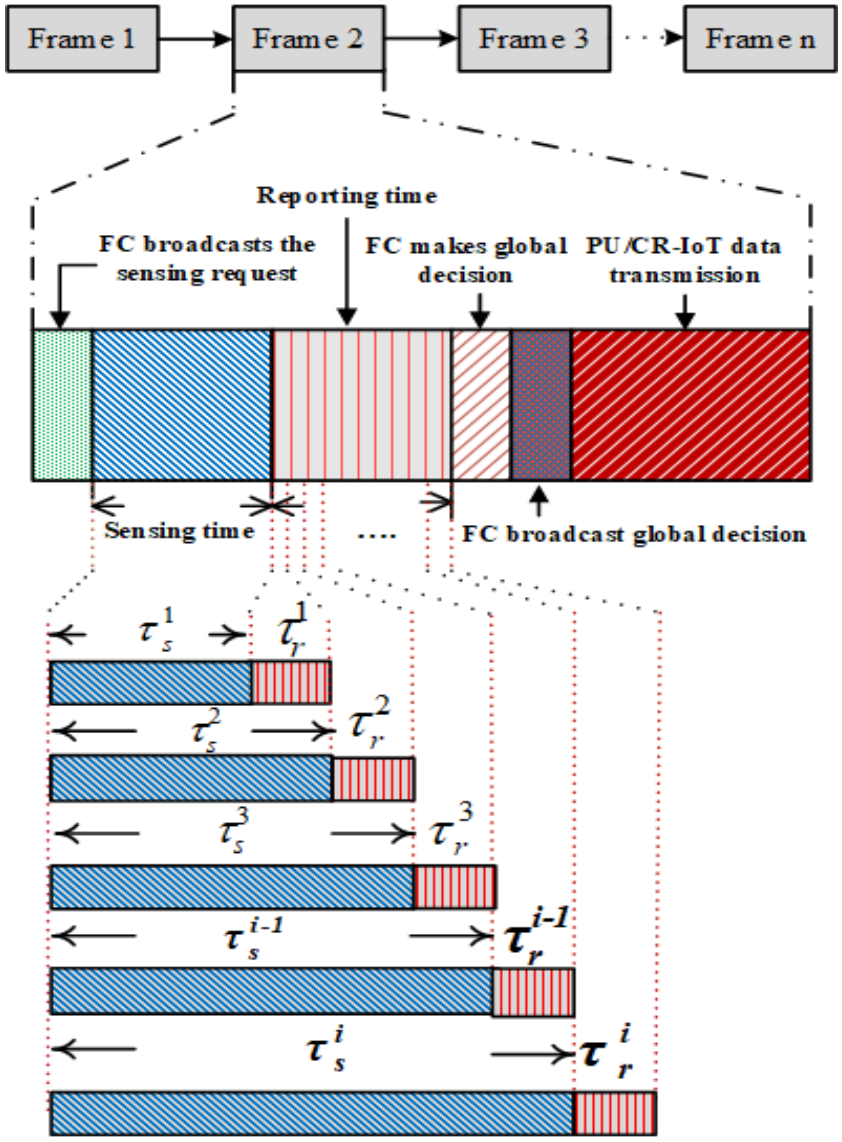

Fig. 4: Packet (i.e., each packet consists of the number of frames) format of the proposed ED method for scenario III where the flexible sensing time slot is obtained based on utilized the reporting framework [2]

4.2 Analysis of Weight Factor using the KLD Award Score

The packet format of the proposed ED method for scenario III where the flexible sensing time slot is obtained based on the reporting framework as depicted in Fig. 4. As a result, based on the flexible sensing time slot, τ_s^p using the

KLD award score, each CR-IoT user to sense the PU licensed spectrum more efficiently.

Now, we can calculate the KLD award score, δ of the proposed ED method using the flexible sensing time slot, τ_s^p with interference constraints for scenario $\mathbb{III}$ which is defined as between the two normally distributed functions $f(\psi)$ and $f^{'}(\psi)$ [5, 50, 51, 59] as follows:

$$\delta\left(f\|f^{'}\right) = \int f(\psi) \times log\left(\frac{f(\psi)}{f^{'}(\psi)}\right) d\psi \tag{16}$$

It is essential to confirm the KLD award score, δ expression of the two Gaussian distributions of $e_i(\mathbb{H}_1)$, and $e_i(\mathbb{H}_0)$ using $\mathbb{H}_1$, and $\mathbb{H}_0$, respectively. Under two hypotheses ($\mathbb{H}_1/\mathbb{H}_0$), the means in Eq. 4 are updated by the flexible sensing time slot (τ_s^p) which are given by

$$\begin{aligned} \bar{\mu}_i\left(\mathbb{H}_0\right) &= 2\tau_s^p f_s \sigma_{z,i}^2 \\ \bar{\mu}_i\left(\mathbb{H}_1\right) &= 4\tau_s^p f_s \left(1 + |h_i|^2 \bar{\gamma}_i\right) \sigma_{z,i}^2 \end{aligned} \tag{17}$$

where $\bar{\mu}_i\left(\mathbb{H}_0\right)$ and $\bar{\mu}_i\left(\mathbb{H}_1\right)$ indicates the updated mean values of the i^{th} CR-IoT user based on the flexible sensing time slot (τ_s^p) under a binary different hypotheses from the previous mean values $\mu_i\left(\mathbb{H}_0\right)$ and $\mu_i\left(\mathbb{H}_0\right)$ in Eq. 4. In addition, $\bar{\gamma}_i$ indicates the Signal to Interference plus Noise Ratio (SINR) that is formulated by $\frac{p_x^2}{(\sigma_{\mathbb{I},i}^2 + \sigma_{x,i}^2)}$; here $\sigma_{\mathbb{I},i}^2$ denotes the PU signal interference power of the i^{th} CR-IoT user.

Similarly, under two hypotheses ($\mathbb{H}_0/\mathbb{H}_1$), the variances in Eq. 4 are updated based on the flexible sensing time slot (τ_s^p) of the proposed ED method which are defined as follows:

$$\begin{aligned} \bar{\sigma}_i^2\left(\mathbb{H}_0\right) &= 2\tau_s^p f_s \sigma_{z,i}^4 \\ \bar{\sigma}_i^2\left(\mathbb{H}_1\right) &= 4\tau_s^p f_s \left(1 + 2|h_i|^2 \bar{\gamma}_i\right) \sigma_{z,i}^4 \end{aligned} \tag{18}$$

where $\bar{\sigma}_i^2\left(\mathbb{H}_0\right)$ and $\bar{\sigma}_i^2\left(\mathbb{H}_0\right)$ represents the updated variance values of the i^{th} CR-IoT user based on the flexible sensing time slot (τ_s^p) under two different hypotheses from the previous variance values $\sigma_i^2\left(\mathbb{H}_0\right)$ and $\sigma_i^2\left(\mathbb{H}_1\right)$ in Eq. 4.

After evaluating the updated means and variances from in Eq. 17 and Eq. 18, each CR-IoT user of the proposed scheme computes the weight factor (Ω_i) based on the KLD award score (δ) using the flexible sensing time slot, τ_s^p is given as follows:

$$\begin{aligned} \Omega_i &= \delta\left(\bar{\mu}_i\left(\mathbb{H}_0\right), \bar{\mu}_i\left(\mathbb{H}_1\right), \bar{\sigma}_i^2\left(\mathbb{H}_0\right), \bar{\sigma}_i^2\left(\mathbb{H}_1\right)\right) \\ &= \frac{1}{2}\left[\log\left(\frac{\bar{\sigma}_i^2\left(\mathbb{H}_0\right)}{\bar{\sigma}_i^2\left(\mathbb{H}_1\right)}\right) - 1 + \left(\frac{\bar{\sigma}_i^2\left(\mathbb{H}_1\right)}{\bar{\sigma}_i^2\left(\mathbb{H}_0\right)}\right) + \frac{\left(\bar{\mu}_i\left(\mathbb{H}_1\right) - \bar{\mu}_i\left(\mathbb{H}_0\right)\right)^2}{\bar{\sigma}_i^2\left(\mathbb{H}_0\right)}\right] \end{aligned} \tag{19}$$

where Ω_i is the weight factor at the i^{th} CR-IoT user of the proposed ED method for scenario $\mathbb{III}$.

4.3 Analysis of Detection Performance

Now, we can estimate the detection probability $p_{d,i}^{\mathbb{III}}$, and the probability of false alarm, $p_{f,i}^{\mathbb{III}}$ of the i^{th} CR-IoT user in the proposed ED scheme for scenario $\mathbb{III}$ by compared to the received signal, e_i with the predetermined local decision threshold, $\lambda_{i,ED}^{\mathbb{III}}$, is given by Eq. 17 and Eq. 18 as follows:

$$\begin{aligned} p_{d,i}^{\mathbb{III}} =& Pr\left[e_i \geq \lambda_{i,ED}^{\mathbb{III}} | \mathbb{H}_1\right] \\ =& \mathbb{Q}\left(\frac{\lambda_{i,ED}^{\mathbb{III}} - \bar{\mu}_i\left(\mathbb{H}_1\right)}{\bar{\sigma}_i^2\left(\mathbb{H}_1\right)}\right) \\ =& \mathbb{Q}\left(\frac{\lambda_{i,ED}^{\mathbb{III}}}{\sqrt{2\tau_s^p f_s(1+2|h_i|^2\bar{\gamma}_i)}\sigma_{z,i}^2} - \frac{\sqrt{2\tau_s^p f_s}\left(1+|h_i|^2\bar{\gamma}_i\right)}{\sqrt{(1+2|h_i|^2\bar{\gamma}_i)}}\right) \end{aligned} \tag{20}$$

and

$$\begin{aligned} p_{f,i}^{\mathbb{III}} = Pr\left[e_i \geq \lambda_{i,ED}^{\mathbb{III}} | \mathbb{H}_0\right] =& \mathbb{Q}\left(\frac{\lambda_{i,ED}^{\mathbb{III}} - \bar{\mu}_i\left(\mathbb{H}_0\right)}{\bar{\sigma}_i^2\left(\mathbb{H}_0\right)}\right) \\ =& \mathbb{Q}\left(\frac{\lambda_{i,ED}^{\mathbb{III}}}{\sqrt{2\tau_s^p f_s}\sigma_{z,i}^2} - \sqrt{2\tau_s^p f_s}\right) \end{aligned} \tag{21}$$

Therefore, the probability of a false alarm, $p_{f,i}^{\mathbb{III}}$ refers to the probability where each CR-IoT user wrongly claims the presence of the PU, though if the PU is really absent on the licensed spectrum for scenario $\mathbb{III}$, whilst the detection probability, $p_{d,i}^{\mathbb{III}}$ refers to the probability where each CR-IoT user correctly claims the presence of the PU, even though the PU is really present on the licensed spectrum for scenario $\mathbb{III}$.

After the sensing phase of the proposed scheme for scenario $\mathbb{III}$, each CR-IoT user forwards its local decision towards the respective FC during the fixed reporting time slot (τ_r), which are integrated with the local decisions in terms of achieving a global decision on the PU's spectrum occupancy. The detection performance at the FC as like the global decision, i.e., $\left(p_{f,FC}^{\mathbb{III}}/p_{d,FC}^{\mathbb{III}}\right)$ based on the weight factor (Ω_i) and the local decision ($p_{f,i}^{\mathbb{III}}/p_{d,i}^{\mathbb{III}}$) of the i^{th} CR-IoT user for scenario $\mathbb{III}$ is calculated by

$$p_{f,FC}^{\mathbb{III}} = \begin{cases} 1, & if \sum_{i=1}^{\mathbb{M}} \Omega_i p_{f,i}^{\mathbb{III}} < \beta^{\mathbb{III}} \\ 0, & otherwise \end{cases} \tag{22}$$

and

$$p_{d,FC}^{\mathbb{III}} = \begin{cases} 1, & if \sum_{i=1}^{\mathbb{M}} \Omega_i p_{d,i}^{\mathbb{III}} \geq \beta^{\mathbb{III}} \\ 0, & otherwise \end{cases} \tag{23}$$

where $\beta^{\mathbb{III}}$ is the global decision threshold at the FC for scenario $\mathbb{III}$.

4.4 Analysis of Sum Rate

After calculating the detection performance at the FC based on the flexible sensing time slot (τ_s^p) in the previous sub-section, now the sum rate is evaluated when considering numerous premises. During the transmission phase, the CR-IoT Tx transmits its own relevant information towards the respective CR-IoT Rx based on round robin scheduling approach [5]. In the case of the non-false alarm, if the PU is absent, each unlicensed CR-IoT user is correctly sensed the absence of the PU; then each unlicensed CR-IoT user is likely to allow the licensed spectrum of the PU for a certain amount of time , as described by the probability of $\left(1 - p_{f,FC}^{\mathbb{III}}\right)$. In another side, in the case of detection, the CR-IoT users should not interfere with the PU transmission. Consequently, the sum rate based on the round robin scheduling approach of the proposed scheme for scenario $\mathbb{III}$ is defined as follows:

$$\mathbb{R}^{\mathbb{III}} = \alpha p_{d,FC}^{\mathbb{III}} \mathbb{R}_{PU}^{\mathbb{III}} + (1-\alpha)\left(1 - p_{f,FC}^{\mathbb{III}}\right) \mathbb{R}_{CR-IoT}^{\mathbb{III}} \tag{24}$$

where $\mathbb{R}^{\mathbb{III}}$ is the sum rate in Hz or b/s, and α is the primary activity factor, that is defined as $\alpha \in [1, 0]$. Moreover, $\mathbb{R}_{CR-IoT}^{\mathbb{III}}$, and $\mathbb{R}_{PU}^{\mathbb{III}}$ are the channel capacity of the CR-IoT link for scenario $\mathbb{III}$, and the channel capacity of the PU link for scenario $\mathbb{III}$, respectively.

Now, we can calculate the channel capacity of the CR-IoT link, $\mathbb{R}_{CR-IoT}^{\mathbb{III}}$, and the channel capacity of the PU link, $\mathbb{R}_{PU}^{\mathbb{III}}$ which are expressed as follows:

$$\mathbb{R}_{CR-IoT}^{\mathbb{III}} = \frac{\mathbb{T} - \tau_s - \tau_r}{\mathbb{T}} \sum_{i=1}^{\mathbb{M}} \mathbb{W} \log_2 \left(1 + \frac{SNR_{CR-IoT,i}}{\mathbb{W}\left(1 + SNR_{PU}\right)}\right) \tag{25}$$

and

$$\mathbb{R}_{PU}^{\mathbb{III}} = \mathbb{W} \log_2 \left(1 + \frac{SNR_{PU}}{\mathbb{W}}\right) \tag{26}$$

where $SNR_{CR-IoT,i}$, $\mathbb{T}$, and SNR_{PU}, indicates the SNR of the CR-IoT $\mathbb{T}$x & the CR-IoT $\mathbb{R}$x link of the i^{th} CR-IoT user, the total frame length, and the SNR of the PU $\mathbb{T}$x and the CR-IoT $\mathbb{R}$x link, respectively.

4.5 Analysis of Spectral Efficiency

Now, the spectral efficiency (SE) of the proposed ED method with interference constraints (scenario $\mathbb{III}$) at the FC is calculated in this sub-section which can be defined as follows:

$$\mathbb{V}_{SE}^{\mathbb{III}} = \frac{\mathbb{R}^{\mathbb{III}}}{\mathbb{W}} \tag{27}$$

where $\mathbb{V}_{SE}^{\mathbb{III}}$ is the SE for scenario $\mathbb{III}$ in b/s/Hz.

4.6 Analysis of Energy Efficiency

In this sub-section, the energy efficiency (EE) of the proposed ED method with interference constraints (scenario $\mathbb{III}$) at the FC is calculated which can defined as follows:

$$\mathbb{V}_{EE}^{\mathbb{III}} = \frac{\mathbb{R}^{\mathbb{III}}}{\mathbb{P}} \tag{28}$$

where $\mathbb{P}$, and $\mathbb{V}_{EE}^{\mathbb{III}}$ indicates the transmit power in J, and the energy efficiency (EE) for scenario $\mathbb{III}$ in b/s/J, respectively.

4.7 Analysis of Global Error Probability

Now, the global error probability, $p_e^{\mathbb{III}}$ of the proposed ED method for scenario $\mathbb{III}$ at the FC is calculated in this sub-section which is given as follows:

$$p_e^{\mathbb{III}} = \alpha p_{f,FC}^{\mathbb{III}} + (1-\alpha)(1-p_{d,FC}^{\mathbb{III}}) \tag{29}$$

4.8 Total Time Analysis

In this sub-section, if the number of CR-IoT users ($\mathbb{M}$) is increased then the total time, $\tau_t^{\mathbb{III}}$ of the proposed ED method for scenario $\mathbb{III}$ is also increased which is consisting of the sum of the fiexed reporting time, τ_r, and the sensing time, τ_s [48]. Therefore, the total time of the proposed ED scheme for scenario $\mathbb{III}$ is defined as follows:

$$\tau_t^{\mathbb{III}} = \tau_s + \sum_{i=1}^{\mathbb{M}} \tau_r^i = \tau_s + \mathbb{M}\tau_r \tag{30}$$

where τ_r^i is the reporting time of the i^{th} CR IoT user i.e., $\tau_r^i = \tau_r$, and $\tau_t^{\mathbb{III}}$ is the total time of the proposed ED scheme for scenario $\mathbb{III}$; here, the reporting time, τ_r and the sensing time, τ_s of the proposed ED method for scenario $\mathbb{III}$ are same, i.e., $\tau_r = \tau_s$.

Therefore, we can see from Eq. 30, the total time, $\tau_t^{\mathbb{III}}$ of the proposed ED method for scenario $\mathbb{III}$ is only depend on the $\mathbb{M}$. If $\mathbb{M}$ is increased by the number of CR-IoT users, the detection performance of the proposed ED method is improved while the total time required is also increased.

The whole idea is demonstrated by the proposed Algorithm 2. In Algorithm 2, it checks $\tau_s^p = \tau_s + M\tau_r$ (see line 8) as the proposed ED scheme for scenario $\mathbb{III}$ is being utilizing the reporting framework. Then it updates the means and variances based on the flexible sensing time slot (τ_s^p) (see line 10/ line 11). Also, it computes the weight factor based on the updated the means and variances (see line 12). Then after that, a global decision, $\left(p_{f,FC}^{\mathbb{III}}/p_{d,FC}^{\mathbb{III}}\right)$ at the FC is computed (see line 14 to 17). Finally, the sum rate, spectral efficiency,

Algorithm 2 The proposed ED method based CSS scheme with interference constraints for scenario $\mathbb{III}$.

Input: $N_s, \mathbb{M}, f_s, \mathbb{T}, \tau_r$, **and** τ_s

Output: Compute the detection probability, $p_{d,FC}^{\mathbb{III}}$**, the probability of a false alarm,** $p_{f,FC}^{\mathbb{III}}$**, the sum rate,** $\mathbb{R}^{\mathbb{III}}$**, the spectral efficiency,** $\mathbb{V}_{SE}^{\mathbb{III}}$**, the energy efficiency,** $\mathbb{V}_{EE}^{\mathbb{III}}$**, and the global error probability,** $p_e^{\mathbb{III}}$

1: Initialize $N_s, \mathbb{M}$
2: **for** i from $\mathbb{M}$ **do**
3: Compute: $e_i = \sum_{l=1}^{N_s} \| z_i \left(\frac{l}{f_s} \right) \|^2$
4: Set: $e_i \sim \begin{cases} \aleph \left(\mu_i \left(\mathbb{H}_0 \right), \sigma_i^2 \left(\mathbb{H}_0 \right) \right); \mu_i \left(\mathbb{H}_0 \right) = 2\tau_s^c f_s \sigma_{z,i}^2 \& \sigma_i^2 \left(\mathbb{H}_0 \right) = 2\tau_s^c f_s \sigma_{z,i}^4 \\ \aleph \left(\mu_i \left(\mathbb{H}_1 \right), \sigma_i^2 \left(\mathbb{H}_1 \right) \right); \mu_i \left(\mathbb{H}_0 \right) = 4\tau_s^c f_s \left(1 + |h_i|^2 \gamma_i \right) \sigma_{z,i}^2 \& \sigma_i^2 \left(\mathbb{H}_0 \right) \\ \qquad\qquad\qquad\qquad = 4\tau_s^c f_s \left(1 + 2|h_i|^2 \gamma_i \right) \sigma_{z,i}^4 \end{cases}$
5: **if** $\mathbb{M} = 1$ **then**
6: Set: $\tau_s^c = \tau_s$
7: Set: $\gamma_i \leftarrow \bar{\gamma}_i$
8: **else**
9: Set: $\tau_s^p = \tau_s + \mathbb{M}\tau_r$
10: Set: $\gamma_i \leftarrow \bar{\gamma}_i$
11: **end if**
12: Calculate: $\bar{\mu}_i \left(\mathbb{H}_0 \right) = 2\tau_s^p f_s \sigma_{z,i}^2$; and $\bar{\mu}_i \left(\mathbb{H}_1 \right) = 4\tau_s^p f_s \left(1 + |h_i|^2 \bar{\gamma}_i \right) \sigma_{z,i}^2$ [using the Eq. 17]
13: Calculate: $\bar{\sigma}_i^2 \left(\mathbb{H}_0 \right) = 2\tau_s^p f_s \sigma_{z,i}^4$; and $\bar{\sigma}_i^2 \left(\mathbb{H}_1 \right) = 4\tau_s^p f_s \left(1 + 2|h_i|^2 \bar{\gamma}_i \right) \sigma_{z,i}^4$ [using the Eq. 18]
14: Calculate: $\Omega_i = \frac{1}{2} \left[\log \left(\frac{\bar{\sigma}_i^2 (\mathbb{H}_0)}{\bar{\sigma}_i^2 (\mathbb{H}_1)} \right) - 1 + \left(\frac{\bar{\sigma}_i^2 (\mathbb{H}_1)}{\bar{\sigma}_i^2 (\mathbb{H}_0)} \right) + \frac{(\bar{\mu}_i (\mathbb{H}_1) - \bar{\mu}_i (\mathbb{H}_0))^2}{\bar{\sigma}_i^2 (\mathbb{H}_0)} \right]$
15: **end for**
16: **if** $\sum_{i=1}^{\mathbb{M}} \Omega_i p_{f,i} < \beta^{\mathbb{III}}$ **then**
17: Set: $p_{f,FC}^{\mathbb{III}} = 1$
18: **else**
19: Set: $p_{f,FC}^{\mathbb{III}} = 0$
20: **end if**
21: **if** $\sum_{i=1}^{\mathbb{M}} \Omega_i p_{d,i} \geq \beta^{\mathbb{III}}$ **then**
22: Set: $p_{d,FC}^{\mathbb{III}} = 1$
23: **else**
24: Set: $p_{d,FC}^{\mathbb{III}} = 0$
25: **end if**
26: Calculate: $\mathbb{R}^{\mathbb{III}} = \alpha p_{d,FC}^{\mathbb{III}} \mathbb{R}_{PU}^{\mathbb{III}} + (1 - \alpha) \left(1 - p_{f,FC}^{\mathbb{III}} \right) \mathbb{R}_{CR-IoT,i}^{\mathbb{III}}$
27: Calculate: $\mathbb{V}_{SE}^{\mathbb{III}} = \frac{\mathbb{R}^{\mathbb{III}}}{\mathbb{W}}$
28: Calculate: $\mathbb{V}_{EE}^{\mathbb{III}} = \frac{\mathbb{R}^{\mathbb{III}}}{\mathbb{P}}$
29: Calculate: $p_e^{\mathbb{III}} = \alpha p_{f,FC}^{\mathbb{III}} + (1 - \alpha)(1 - p_{d,FC}^{\mathbb{III}})$

energy efficiency, and global error probability is computed based on the global detection ($p_{f,FC}^{\mathbb{III}}/p_{d,FC}^{\mathbb{III}}$) at the FC (see lines from 24 to 27).

Table 3: **Simulation parameters are summarized that are required.**

Parameter	**Value in unit**
The number of CR-IoT users, $\mathbb{M}$	14
The sampling frequency, f_s	350 kHz
The flexible sensing time slot, τ_s^p	10 ms
The reporting time slot, τ_r	5 ms
The non-flexible sensing time slot, τ_s^c	5 ms
SNR_{PU}	12 dB
$SNR_{CR-IoT,i}$	8 dB
The PU transmitted signal, $s(k)$	BPSK
The number of samples, N_s	25
Global decision threshold, β	3
The PU activity factor, α	0.7

5 Simulation Results and Discussion

The simulation findings with the relevant explanation is discussed in this section. Numerical assessments were carried out and contrasted with those of many other conventional ED methods employing Monte Carlo test to evaluate the detection probability of the proposed ED method. MATLAB R2020b is used to run simulations, and the findings are computed from an average of $20 \times 10^3 - 50 \times 10^3$ independent simulation loops. Table 3 summarizes the simulation parameters that are required.

First for scenario $\mathbb{I}$, the detection performance of the conventional ED method, and the proposed ED method are evaluated; then, their performance is depicted in Fig. 5a. The performance achieved when the SNR, i.e.,γ is -4dB, the predetermined sample, N_x) is 25, the flexible sensing time slot, τ_s^p is $10ms$, and the non-flexible sensing time slot, τ_s^c is $5ms$. The cooperative detection performance is drawn by Receiver Operating Characteristic (ROC) curves for the proposed ED method, and the conventional ED method for scenario $\mathbb{I}$ under the flexible and non-flexible sensing time slots which is shown in Fig. 5a. In τ_s^p, the detection probability of the conventional scheme is an enhanced. For instance, if $p_{f,FC}^{\mathbb{I}}$ is 0.20 for the conventional ED method for scenario $\mathbb{I}$, then the detection probability, $p_{d,FC}^{\mathbb{I}}$ under the non-flexible sensing time slot ($\tau_s^c = 5ms$), and the probability of detection, $p_{d,FC}^{\mathbb{I}}$ under the flexible sensing time slot ($\tau_s^p = 10ms$) are 0.60 and 0.65, respectively. Similarly, if $p_{f,FC}^{\mathbb{I}}$ is 0.20 for the proposed ED method for scenario $\mathbb{I}$, then the detection probability, $p_{d,FC}^{\mathbb{I}}$ under the non-flexible sensing time slot ($\tau_s^c = 5ms$), and the detection probability, $p_{d,FC}^{\mathbb{I}}$ under the flexible sensing time slot ($\tau_s^p = 10ms$) are 0.89 and 0.94, respectively. Because of the weighted factor, Ω_i, the detection performance is improved in the proposed ED method for scenario $\mathbb{I}$. In an FC, both the ROCs in the conventional ED method, and the proposed ED method can be compared where the proposed ED method has a much

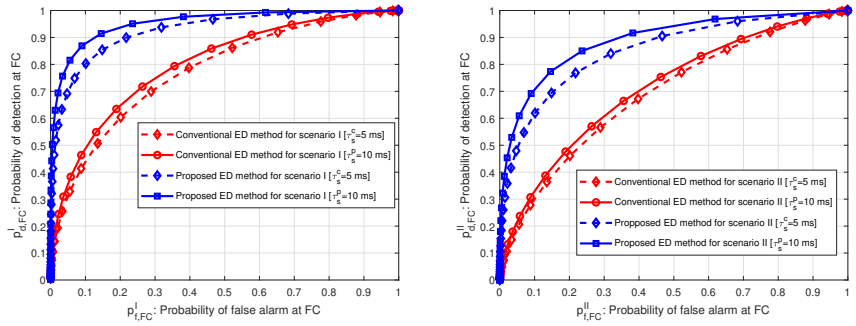

(a) $p^{\mathbb{I}}_{d,FC}$ vs. $p^{\mathbb{I}}_{f,FC}$ for scenario $\mathbb{I}$ (b) $p^{\mathbb{III}}_{d,FC}$ vs. $p^{\mathbb{III}}_{f,FC}$ for scenario $\mathbb{III}$

Fig. 5: The ROC curves for the proposed ED method, and the conventional ED method when both scenario $\mathbb{I}$, and $\mathbb{III}$ are considered.

better detection performance (29% when $\tau_s^c = 5ms$ and $\tau_s^p = 10ms$) than the conventional ED method for scenario $\mathbb{I}$.

Fig. 5b illustrates the ROC curve of the cooperative detection performance obtained based on different sensing time slots, i.e., τ_s^c, and τ_s^p, of the proposed ED method and the conventional ED method with interference constraints for scenario $\mathbb{III}$. Within the flexible sensing time slot, τ_s^p of the conventional ED method, the detection probability enhances as shown in Fig. 5b. For instance, if $p^{\mathbb{III}}_{f,FC}$ is 0.20 of the conventional ED method for scenario $\mathbb{III}$, then the detection probability, $p^{\mathbb{III}}_{d,FC}$ with fixed sensing time slot ($\tau_s^c = 5ms$), and the detection probability, $p^{\mathbb{III}}_{d,FC}$ with flexible sensing time slot ($\tau_s^p = 10ms$) are 0.48 and 0.50, respectively. Similarly, if $p^{\mathbb{III}}_{f,FC}$ is 0.20 of the proposed ED method for scenario $\mathbb{III}$, then the probability of detection, $p^{\mathbb{III}}_{d,FC}$ with fixed sensing time slot ($\tau_s^c = 5ms$), and the detection probability, $p^{\mathbb{III}}_{d,FC}$ with flexible sensing time slot ($\tau_s^p = 10ms$) are 0.78 and 0.81, respectively. Because of the weighted factor, Ω_i of the proposed ED method for scenario $\mathbb{III}$, the detection performance is an improved in the proposed scheme. It is clearly seen in the proposed ED method and the conventional ED method by contrasting all ROCs at the FC where the proposed ED method has a much better detection performance (31% when $\tau_s^c = 5ms$ and 30% when $\tau_s^p = 10ms$) than the conventional ED method for scenario $\mathbb{III}$.

At the FC, by comparison of the detection performance is shown in Fig. 5a as well as Fig. 5b; here, both are demonstrated that with $\tau_s^c = 5$ ms, the proposed ED method for scenario $\mathbb{I}$ is detected the licensed PU's spectrum with 89% detection performance, while the conventional ED method for scenario $\mathbb{I}$ is detected the licensed PU's spectrum with 60% detection performance that is listed in Table 4.

Fig. 6 shows the detection probability, and the probability of false alarm of the proposed ED method versus SNR for scenarios $\mathbb{I}$, where $N = 20$ and $\tau_s = 10$ms and $\tau_r = 5$ ms. We can seen from Fig. 6a, the detection perfor-

Table 4: **Detection performance of the proposed ED method, and the conventional ED method at a FC, when both scenario $\mathbb{I}$, and scenario $\mathbb{III}$ are considered; here, the probability of false alarm $(p^{\mathbb{I}}_{f,FC} = p^{\mathbb{III}}_{f,FC})$ is** 0.20**.**

Schemes e.g., detection probability	$\tau^c_s = 5ms$	$\tau^p_s = 10ms$
The conventional ED method for scenario $\mathbb{I}$	0.60	0.65
The proposed ED method for scenario $\mathbb{I}$	0.89	0.94
The conventional ED method for scenario $\mathbb{III}$	0.50	0.57
The proposed ED method for scenario $\mathbb{III}$	0.82	0.89

mance of the proposed ED method increases significantly as the SNR value are increasing.

For instance, for $N_s = 20$, the probability of detection is 44% when $SNR = -9$dB, 68% when $SNR = -6$dB, and 90% when $SNR = -3$dB; whereas the detection performance of the conventional scheme slightly increases as SNR value increases. Again for instance, for the conventional ED scheme with $N_s = 20$, the probability of detection achieves 0% for $SNR = -9$dB, 5% for $SNR = -6$dB, and 15% for $SNR = -3$dB. Furthermore, we seen that the $p^{\mathbb{I}}_{f,FC}$ of the proposed ED method significantly decreases as the SNR value increases as depicted in Fig. 6b. However, we clearly seen from this simulation where the detection performance of the conventional ED method did not perform well whereas the SNR value is -8 dB. Therefore, it is seen that the conventional ED method is not sufficient for low SNR value, i.e., $SNR \leq -8$ dB.

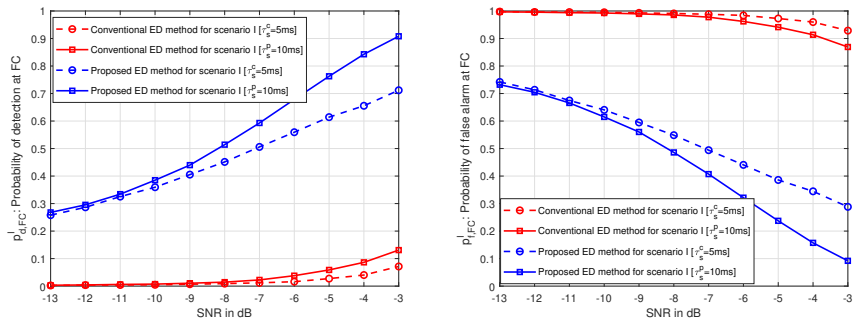

(a) SNR vs. $p^{\mathbb{I}}_{d,FC}$ for scenario $\mathbb{I}$ (b) SNR vs. $p^{\mathbb{I}}_{f,FC}$ for scenario $\mathbb{I}$

Fig. 6: SNR vs. the detection probability, and the probability of false alarm at FC when scenario $\mathbb{I}$ is only considered.

Fig. 7 demonstrates probability of false alarm, and the detection probability of the proposed ED method versus the SINR value for scenario $\mathbb{III}$, where $N = 20$ and $\tau^p_s = 10$ms and $\tau_r = 5$ ms. We can seen that the probability of detection of the proposed ED method significantly increases when the $SINR$

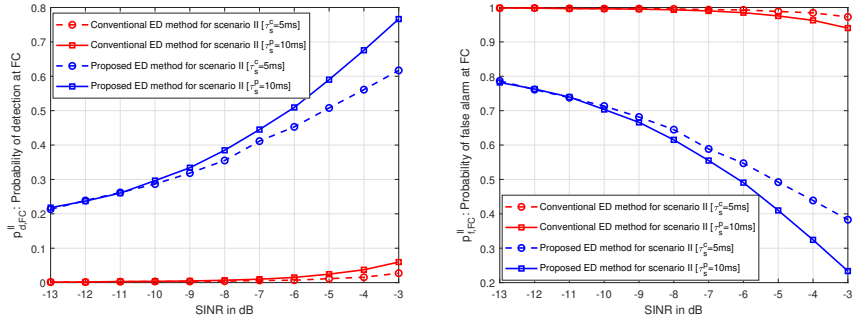

(a) SINR vs the detection probability for scenario $\mathbb{III}$

(b) SINR vs the probability of false alarm for scenario $\mathbb{III}$

Fig. 7: $SINR$ vs. the detection probability, and the probability of false alarm at FC when scenario $\mathbb{III}$ is only considered.

value is increasing as shown in Fig. 7a. For example, the detection probability is 35% when $SINR = -9$dB, 51% when $SINR = -6$dB, and 78% when $SINR = -3$dB; whereas the detection probability of the conventional ED scheme slightly increases with increasing $SINR$. For example, for $N_s = 20$, the detection probability is 0% when $SINR = -9$dB, 4% when $SINR = -6$dB, and 8% when $SINR = -3$dB. Moreover, according to Fig. 7b, we have seen it with increasing SINR, then the $p_{f,FC}^{\mathbb{III}}$ of the proposed ED method is decreased. For example, for $N_s = 20$, the $p_{f,FC}^{\mathbb{III}}$ is 68% when $SINR = -9$dB, 48% when $SINR = -6$dB, and 20% when $SINR = -3$dB; whereas the $p_{f,FC}^{\mathbb{III}}$ of the conventional ED method slightly decreases when the $SINR$ value is increasing. For example, for $N_s = 20$, the $p_{f,FC}^{\mathbb{III}}$ is 100% when $SINR = -9$dB, 98% when $SINR = -6$dB, and 92% when $SINR = -3$dB. However, we can see from this simulation where the detection performance of the conventional ED method did not perform well when the $SINR$ value is -8 dB. Therefore, it is seen that the conventional ED scheme did not perform well when the low $SINR$ value is considered i.e., $SINR \leq -8$ dB.

Fig. 8a demonstrates the sum rates of the proposed ED method, and the conventional ED method without interference constraints for scenario $\mathbb{I}$ that depends on the $p_{f,FC}^{\mathbb{I}}$. The sum rate of the proposed ED method for scenario $\mathbb{I}$ is better when compared with the conventional ED method for the whole value of the $p_{f,FC}^{\mathbb{I}}$. Consequently, the sum rate ROC defines a quasi concave function of the $p_{f,FC}^{\mathbb{I}}$ for the PU activity factor (α). As a result, for the scenario $\mathbb{I}$, the sum rate of the proposed ED method achieved $2360Hz$, while the sum rate of the conventional ED method achieved $1921Hz$ under the non-flexible sensing time slot ($\tau_s^c = 5ms$), the number of samples ($N_s = 20$), and the $p_{f,FC}^{\mathbb{I}} = 0.2$ as shown in Fig. 8a. Moreover, the sum rate of the proposed ED method, and the conventional ED method for scenario $\mathbb{I}$ under the number of samples ($N_s = 20$), the flexible sensing time slot ($\tau_s^p = 10ms$), and the probability of

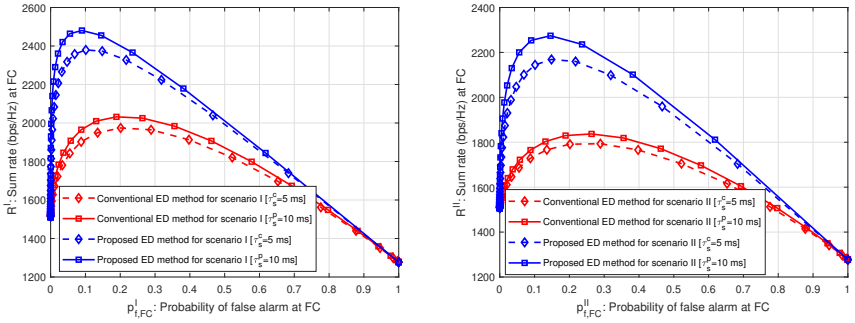

(a) $\mathbb{R}^{\mathbb{I}}$ vs. $p^{\mathbb{I}}_{f,FC}$ for scenario $\mathbb{I}$ (b) $\mathbb{R}^{\mathbb{III}}$ vs. $p^{\mathbb{III}}_{f,FC}$ for scenario $\mathbb{III}$

Fig. 8: Sum rate curves at FC of the conventional ED method, and the proposed ED method when scenario $\mathbb{I}$, scenario $\mathbb{III}$, and $\alpha = 0.7$ are considered.

false alarm ($p^{\mathbb{I}}_{f,FC}$) are 2500 Hz, and 2000 Hz, respectively. Therefore, we argue that as compared to the sum rate of the conventional ED method with the number of samples ($N_s = 20$), and the non-flexible sensing time slot ($\tau^c_s = 5$) ms or the flexible sensing time slot ($\tau^p_s = 10$) ms; the sum rate of the proposed ED method for scenario $\mathbb{I}$ is an enhanced.

Fig. 8b shows the sum rates of the proposed ED method, and conventional ED method with scenario $\mathbb{III}$ depends on the probability of false alarm which is a function of the $p^{\mathbb{III}}_{f,FC}$. For the entire range of the $p^{\mathbb{III}}_{f,FC}$, the sum rate of the proposed ED method achieved a higher compared to the conventional ED method. Therefore, the sum rate of the proposed ED method for scenario $\mathbb{III}$ achieved $2149Hz$, whilst the sum rate of the conventional ED technique achieved $1700Hz$ when the non-flexible sensing time slot ($\tau^c_s = 5ms$), the number of samples ($N_s = 20$), and the probability of false alarm ($p^{II}_{f,FC} = 0.2$). Moreover, the sum rate of the conventional ED method for scenario $\mathbb{III}$ is $1792Hz$, whilst the sum rate of the proposed ED method is $2280Hz$ at the probability of false ($p^{\mathbb{III}}_{f,FC} = 0.2$) with the number of samples ($N_s = 20$) and the flexible sensing time slot ($\tau_s = 10ms$). Therefore, we argue that as compared to the sum rate of the conventional ED method when the number of samples ($N_s = 20$), and the no-flexible sensing time slot ($\tau^c_s = 5ms$) or the flexible sensing time slot ($\tau^p_s 10ms$) for scenario $\mathbb{III}$, the sum rate of the proposed ED method achieved an enhanced.

The spectral efficiency of the conventional ED method and the proposed ED method demonstrates in Fig. 9 when both scenario $\mathbb{I}$ and scenario $\mathbb{III}$ are considered. For scenario $\mathbb{I}$, the spectral efficiency of the proposed ED method achieved a better when compared to the conventional ED method due to its higher sum rate as shown in Fig. 9a. Here, we clearly seen as the $\mathbb{V}^{\mathbb{I}}_{SE}$ of the proposed ED method ($8.4bps/Hz$) achieved a higher compared with the conventional ED method ($6.5bps/Hz$), where $p^{I}_{f,FC}$ is 0.1, and the sensing time slot (τ^p_s) is $10ms$ for scenario $\mathbb{I}$. Similarly, the spectral efficiency of the

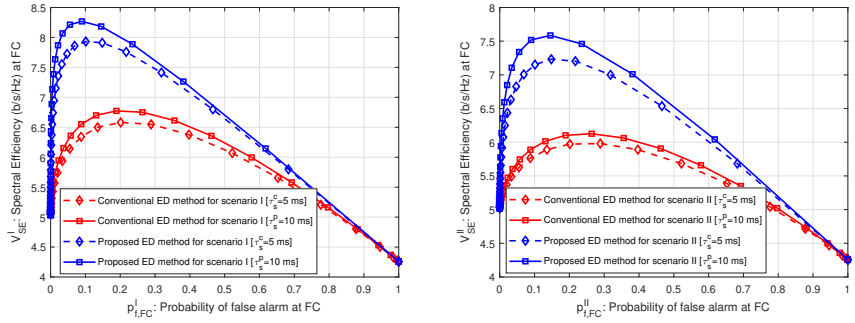

(a) SE vs. $p_{f,FC}^{\mathbb{I}}$ for scenario $\mathbb{I}$ (b) SE vs. $p_{f,FC}^{\mathbb{III}}$ for scenario $\mathbb{III}$

Fig. 9: Spectral efficiency curves at FC of the conventional ED method and the proposed ED method when both scenario $\mathbb{I}$ and scenario $\mathbb{III}$ are considered.

proposed ED method ($7.5bps/Hz$) obtained a higher compared by the conventional ED method ($5.8bps/Hz$) for scenario $\mathbb{III}$, where $p_{f,FC}^{\mathbb{III}}$ is 0.1, and the sensing time slot (τ_s^p) is $10ms$ as shown in Fig. 9b. Therefore, we argue that the $\mathbb{V}_{SE}^{\mathbb{III}}$ of the proposed ED method ($7.5bps/Hz$) for scenario $\mathbb{III}$ obtained a lower compared with the proposed ED method ($8.4bps/Hz$) for scenario $\mathbb{I}$ due to the interference constraints is considering in scenario $\mathbb{III}$ which degrades the detection performance of the PU spectrum.

In Fig. 10, it demonstrates the energy efficiency of the conventional ED method, and the proposed ED method when both scenarios are considered, i.e., $\mathbb{I}$, and $\mathbb{III}$. For scenario $\mathbb{I}$, the energy efficiency of the proposed ED method achieved a higher compared to the conventional ED method because of its higher sum rate as shown in Fig. 10a. Here for scenario $\mathbb{I}$, we clearly seen that the energy efficiency of the proposed ED method ($1.30bps/J$) is a better when compared to the conventional ED method ($1.04bps/J$), where the flexible sensing time slot (τ_s^p), and the probability of false alarm ($p_{f,FC}^{\mathbb{I}}$) are $10ms$, and 0.1, respectively. Similarly for scenario $\mathbb{III}$, the energy efficiency of the proposed ED method ($1.2bps/J$) is a better when compared to the conventional ED method ($0.94bps/J$), where the sensing time slot (τ_s^p) is $10ms$, and $p_{f,FC}^{\mathbb{III}}$ is 0.1. Finally, we argue that the energy efficiency of the proposed ED method for scenario $\mathbb{III}$ achieved a lower compared with the proposed ED method with scenario $\mathbb{I}$ due to the scenario $\mathbb{III}$ is considering the interference constraints which degrades the detection performance.

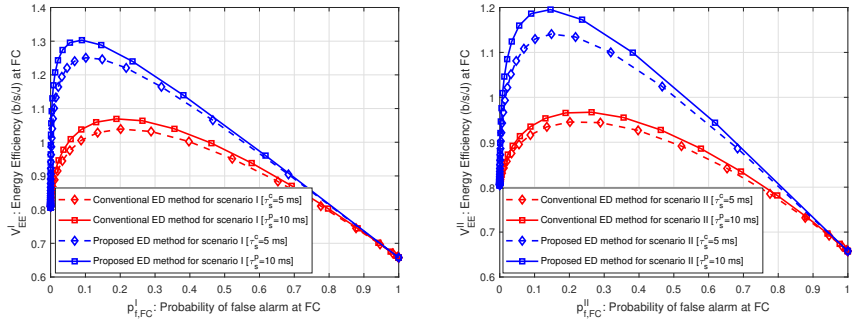

(a) Energy efficiency vs. $p_{f,FC}^{\mathbb{I}}$ under scenario $\mathbb{I}$ (b) Energy efficiency vs. $p_{f,FC}^{\mathbb{III}}$ under scenario $\mathbb{III}$

Fig. 10: Energy efficiency curves vs. the probability of false alarm at FC for the conventional ED method, and the proposed ED method when scenario $\mathbb{I}$ and scenario $\mathbb{III}$ are considered.

Fig. 11 shows the global error probability for the conventional ED method, and the proposed ED method when scenario $\mathbb{I}$ and scenario $\mathbb{III}$ are considered. We shown in Fig. 11a, the global error probability for both the proposed ED method and the conventional ED method decreases as the probability of false alarm decreases as like 0.3 to 0.0.

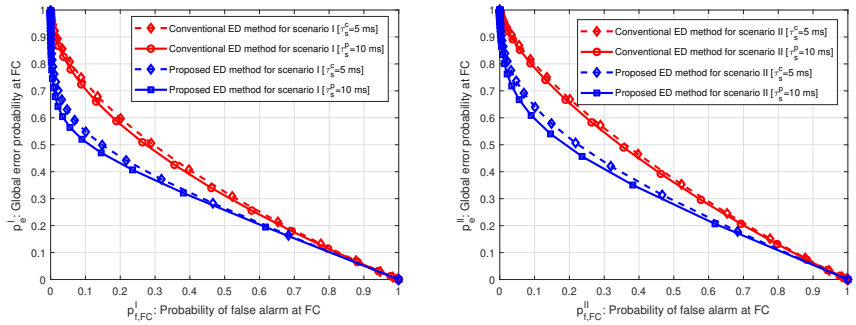

(a) Global error probability curves versus $p_{f,FC}^{\mathbb{I}}$ at FC for scenario $\mathbb{I}$ (b) Global error probability curves versus $p_{f,FC}^{\mathbb{III}}$ at FC for scenario $\mathbb{III}$

Fig. 11: Global error probability curves at FC of the conventional ED method and the proposed ED method when scenario $\mathbb{I}$ and scenario $\mathbb{III}$ are considered.

Therefore, in terms of the global error probability for scenario $\mathbb{I}$, the proposed ED method achieves 50% compared to 70% with the conventional scheme at $p_{f,FC}^{\mathbb{I}} = 0.1$, when the sensing time slot (τ_s^p) is $10ms$. Similarly, we observed from Fig. 11b, it is clearly seen as the $p_e^{\mathbb{III}}$ of the proposed ED method for sce-

nario $\mathbb{III}$ achieves 60% compared to 80% with the conventional ED method at $p_{f,FC}^{\mathbb{III}} = 0.1$, when the sensing time slot (τ_s^p) is $10ms$. Therefore, we conclude from Fig. 11a and Fig. 11b, in terms of the global error probability, the proposed ED method (60%) for scenario $\mathbb{III}$ achieves a higher compared to the proposed ED method (50%) for scenario $\mathbb{I}$ due to the interference constraints is considering in scenario $\mathbb{III}$ which also degrades the global error probability.

6 Conclusion

The detection performance of the conventional ED method and the proposed ED method for CSS scheme has been presented. In the detection performance, (i) for scenario $\mathbb{I}$, the proposed ED method with the flexible sensing time slot i.e., τ_s^p demonstrates a 8%, 38% and 47% improvement over the proposed ED method with the non-flexible sensing time slot e.g, τ_s^c, the conventional ED method with the flexible sensing time slot, e.g, τ_s^p and the conventional ED method with the non-flexible sensing time slot, i.e., τ_s^c, respectively; and (ii) for scenario $\mathbb{III}$, the proposed ED method with flexible sensing time slot demonstrates a 10%, 43% and 46% improvement over the proposed ED method with non-flexible sensing time slot, the conventional ED method with flexible sensing time slot, and the conventional ED method with non-flexible sensing time slot, respectively. Also, with respect to sum rate, (i) for scenario $\mathbb{I}$, the proposed ED method with flexible sensing time slot demonstrates a 7%, 45%, and 53% improvement over the proposed ED method with non-flexible sensing time slot, the conventional ED method with flexible sensing time slot, and the conventional ED method with non-flexible sensing time slot, respectively; and (ii) for scenario $\mathbb{III}$, the proposed ED method with flexible sensing time slot demonstrates a 11%, 49%, and 54% improvement over the proposed ED method with non-flexible sensing time slot, the conventional ED method with flexible sensing time slot, and the conventional ED method with non-flexible sensing time slot, respectively. In terms of bandwidth of the spectral efficiency, (i) for scenario $\mathbb{I}$, the proposed ED method with flexible sensing time slot, demonstrates a 5%, 17%, and 19% improvement over the proposed ED method with non-fixed sensing time slot, the conventional ED method with flexible sensing time slot, and the conventional ED method with non-flexible sensing time slot, respectively; and (ii) for scenario $\mathbb{III}$, the proposed ED method with flexible sensing time slot demonstrates a 3%, 17% and 20% improvement over the proposed ED method with non-flexible sensing time slot, the conventional ED method with flexible sensing time slot, and the conventional ED method with non-flexible sensing time slot, respectively. In addition, in terms of sum rate of the energy efficiency, (i) for scenario $\mathbb{I}$, the proposed ED method with flexible sensing time slot demonstrates a 3%, 18% and 20% better over the proposed ED method with non-flexible sensing time slot, the conventional ED method with flexible sensing time slot, and the conventional ED method with non-flexible sensing time slot, respectively; and (ii) for scenario $\mathbb{III}$, the proposed ED method with flexible sensing time slot demonstrates

a 3%, 24%, and 26% improvement over the proposed ED method with non-flexible sensing time slot, the conventional ED method with flexible sensing time slot, and the conventional ED method with non-flexible sensing time slot, respectively. Eventually, a global error probability of 50% obtains in the proposed ED method with flexible sensing time slot for scenario $\mathbb{I}$, while 56%, 70%, and 72% global error probabilities obtains in the proposed ED method with non-flexible sensing time slot, the conventional ED method with flexible sensing time slot, and the conventional ED method with non-flexible sensing time slot, where $p^{\mathbb{I}}_{f,FC}$ is 0.1. Moreover, the global probability error of 60% obtains in the proposed ED method based on the flexible sensing time slot for scenario $\mathbb{III}$, while 66%, 80% and 81% global error probabilities obtains in the proposed ED method with non-flexible sensing time slot, the conventional ED method with flexible sensing time slot, and the conventional ED method with non-flexible sensing time slot, where $p^{\mathbb{III}}_{f,FC}$ is 0.1.

In the proposed ED method, the dynamic threshold will be considered under a real time environment in our future work.

Declarations

Funding
This research was supported in part by the Department of Information and Communication Technology, Islamic University, Kushtia-7003, Bangladesh and by the Ministry of Science and Technology, Bangladesh.

Conflicts of interest
The authors declare that they have no conflicts of interest.

Availability of data and material
Not applicable.

Code availability
Not applicable.

References

1. Yu, H., Lee, H., & Jeon, H. (2017). What is 5G? Emerging 5G mobile services and network requirements. *Sustainability*, 9(10), 1848.
2. Miah, M. S., Schukat, M., & Barrett, E. (2018). An enhanced sum rate in the cluster based cognitive radio relay network using the sequential approach for the future Internet of Things. *Human-centric Computing and Information Sciences*, 8(1), 1-27.
3. Zhu, J., Song, Y., Jiang, D., & Song, H. (2017). A new deep-Q-learning-based transmission scheduling mechanism for the cognitive Internet of Things. *IEEE Internet of Things Journal*, 5(4), 2375-2385.
4. Li, T., Yuan, J., & Torlak, M. (2018). Network throughput optimization for random access narrowband cognitive radio Internet of Things (NB-CR-IoT). *IEEE Internet of Things Journal*, 5(3), 1436-1448.
5. Miah, M. S., Schukat, M., & Barrett, E. (2020). Sensing and throughput analysis of a MU-MIMO based cognitive radio scheme for the Internet of Things. *Computer Communications*, 154, 442-454.

6. Kim, B., Yu, H., & Noh, S. (2020). Cognitive interference cancellation with digital channelizer for satellite communication. *Sensors*, 20(2), 355.
7. Awin, F. A., Alginahi, Y. M., Abdel-Raheem, E., & Tepe, K. (2019). Technical issues on cognitive radio-based Internet of Things systems: A survey. *IEEE Access*, 7, 97887-97908.
8. Tang, Y., & Li, Q. (2011). Reviews on the Cognitive Radio Platform Facing the IOT. *In Informatics in Control, Automation and Robotics*, (pp. 825-833), Springer, Berlin, Heidelberg.
9. Khan, A. A., Rehmani, M. H., & Rachedi, A. (2017). Cognitive-radio-based internet of things: Applications, architectures, spectrum related functionalities, and future research directions. *IEEE wireless communications*, 24(3), 17-25.
10. ÇAVDAR, T., & Ebrahimpour, N. (2019). Decision-making for small industrial Internet of Things using decision fusion. *Turkish Journal of Electrical Engineering & Computer Sciences*, 27(6), 4134-4150.
11. Chen, Y. K. (2012, January). Challenges and opportunities of internet of things. *In 17th Asia and South Pacific design automation conference* (pp. 383-388). IEEE.
12. Amjad, M., Rehmani, M. H., & Mao, S. (2018). Wireless multimedia cognitive radio networks: A comprehensive survey. *IEEE Communications Surveys & Tutorials*, 20(2), 1056-1103.
13. Wang, B., & Liu, K. R. (2010). Advances in cognitive radio networks: A survey. *IEEE Journal of selected topics in signal processing*, 5(1), 5-23.
14. Amin, M. R., Rahman, M. M., Hossain, M. A., Islam, M. K., Ahmed, K. M., Singh, B. C., & Miah, M. S. (2018). Unscented kalman filter based on spectrum sensing in a cognitive radio network using an adaptive fuzzy system. *Big Data and Cognitive Computing*, 2(4), 39.
15. Mitola, J., & Maguire, G. Q. (1999). Cognitive radio: making software radios more personal. *IEEE personal communications*, 6(4), 13-18.
16. Haykin, S. (2005). Cognitive radio: brain-empowered wireless communications. *IEEE journal on selected areas in communications*, 23(2), 201-220.
17. Wyglinski, A. M., Nekovee, M., & Hou, T. (Eds.). (2009). Cognitive radio communications and networks: principles and practice. *Academic Press*.
18. Alghorani, Y., Kaddoum, G., Muhaidat, S., Pierre, S., & Al-Dhahir, N. (2015). On the performance of multihop-intervehicular communications systems over n* Rayleigh fading channels. *IEEE Wireless Communications Letters*, 5(2), 116-119.
19. Joshi, P., & Bagwari, A. (2019). An overview of cognitive radio networks: A future wireless technology. *Sensing Techniques for Next Generation Cognitive Radio Networks*, 1-26.
20. Supraja, P., Gayathri, V. M., & Pitchai, R. (2019). Optimized neural network for spectrum prediction using genetic algorithm in cognitive radio networks. *Cluster Computing*, 22(1), 157-163.
21. Gu, Y., Chen, H., Zhai, C., Li, Y., & Vucetic, B. (2019). Minimizing age of information in cognitive radio-based iot systems: Underlay or overlay?. *IEEE Internet of Things Journal*, 6(6), 10273-10288.
22. Majumder, S. (2018, October). Energy detection spectrum sensing on RTL-SDR based IoT platform. *In 2018 Conference on Information and Communication Technology (CICT)* (pp. 1-6). IEEE.
23. Mayekar, N., & Wyglinski, A. M. (2015, May). Interference performance evaluation of secondary users in cognitive radio networks. *In 2015 IEEE 81st Vehicular Technology Conference (VTC Spring)* (pp. 1-5). IEEE.
24. Hossain, M. A., Schukat, M., & Barrett, E. (2020). Enhancing the spectrum sensing performance of cluster-based cooperative cognitive radio networks via sequential multiple reporting channels. *Wireless Personal Communications*, 1-23.
25. Semba Yawada, P., & Trung Dong, M. (2018). Performance analysis of new spectrum sensing scheme using multiantennas with multiuser diversity in cognitive radio networks. *Wireless Communications and Mobile Computing*, 2018.
26. Lu, D., Huang, X., Zhang, W., & Fan, J. (2014). Interference-aware spectrum handover for cognitive radio networks. *Wireless Communications and Mobile Computing*, 14(11), 1099-1112.

27. Miah, M., Ahmed, K. M., Islam, M., Mahmud, M., Raihan, A., Rahman, M., & Yu, H. (2020). Enhanced sensing and sum-rate analysis in a cognitive radio-based internet of things. *Sensors*, 20(9), 2525.
28. Hassan, Y., El-Tarhuni, M., & Assaleh, K. (2012). Learning-based spectrum sensing for cognitive radio systems. *Journal of Computer Networks and Communications*, 2012.
29. Nadeem, A., Khan, M., & Han, K. (2017). Non-cooperative spectrum sensing in context of primary user detection: A review. *IETE Technical Review*, 34(2), 188-200.
30. Akyildiz, I. F., Lee, W. Y., Vuran, M. C., & Mohanty, S. (2006). NeXt generation/dynamic spectrum access/cognitive radio wireless networks: A survey. *Computer networks*, 50(13), 2127-2159.
31. Nguyen, V. D., & Shin, O. S. (2017). Cooperative prediction and sensing based spectrum sharing in cognitive radio networks. *IEEE Transactions on Cognitive Communications and Networking*, 4(1), 108-120.
32. Vimal, S., Kalaivani, L., & Kaliappan, M. (2019). Collaborative approach on mitigating spectrum sensing data hijack attack and dynamic spectrum allocation based on CASG modeling in wireless cognitive radio networks. *Cluster Computing*, 22(5), 10491-10501.
33. El-Saleh, A. A., Ismail, M., Ali, M. A. M., & Arka, I. H. (2010). Hybrid SDF-HDF cluster-based fusion scheme for cooperative spectrum sensing in cognitive radio networks. *KSII Transactions on Internet and Information Systems (TIIS)*, 4(6), 1023-1041.
34. Shen, B., & Kwak, K. S. (2009). Soft combination schemes for cooperative spectrum sensing in cognitive radio networks. *ETRI journal*, 31(3), 263-270.
35. Bouraoui, R., & Besbes, H. (2016, September). Cooperative spectrum sensing for cognitive radio networks: Fusion rules performance analysis. *In 2016 International wireless communications and mobile computing conference (IWCMC)* (pp. 493-498). IEEE.
36. Ahmed, M. E., Kim, D. I., Kim, J. Y., & Shin, Y. (2017). Energy-arrival-aware detection threshold in wireless-powered cognitive radio networks. *IEEE Transactions on Vehicular Technology*, 66(10), 9201-9213.
37. Tavana, M., Rahmati, A., Shah-Mansouri, V., & Maham, B. (2016). Cooperative sensing with joint energy and correlation detection in cognitive radio networks. *IEEE Communications Letters*, 21(1), 132-135.
38. Miah, M. S., & Rahman, M. M. (2014, April). An eigenvalue and superposition approach based cooperative spectrum sensing in cognitive radio networks. *In 2014 international conference on electrical engineering and information & communication technology* (pp. 1-7). IEEE.
39. Plata, D. M. M., & Reátiga, Á. G. A. (2012). Evaluation of energy detection for spectrum sensing based on the dynamic selection of detection-threshold. *Procedia Engineering*, 35, 135-143.
40. Khan, R. T., Islam, M. I., Zaman, S., & Amin, M. R. (2016, December). Comparison of cyclostationary and energy detection in cognitive radio network. *In 2016 International Workshop on Computational Intelligence (IWCI)* (pp. 165-168). IEEE.
41. Sarala, B., Devi, D. R., & Bhargava, D. S. (2019). Classical energy detection method for spectrum detecting in cognitive radio networks by using robust augmented threshold technique. *Cluster Computing*, 22(5), 11109-11118.
42. Hossain, M. A., Schukat, M., & Barrett, E. (2019, June). Enhancing the spectrum utilization in cellular mobile networks by using cognitive radio technology. *In 2019 30th Irish signals and systems conference (ISSC)* (pp. 1-6). IEEE.
43. Kang, B. J. (2009, September). Spectrum sensing issues in cognitive radio networks. *In 2009 9th international symposium on communications and information technology* (pp. 824-828). IEEE.
44. Kobeissi, H., Nasser, Y., Nafkha, A., Bazzi, O., & Louet, Y. (2016). On the detection probability of the standard condition number detector in finite-dimensional cognitive radio context. *EURASIP Journal on Wireless Communications and Networking*, 2016(1), 1-11.
45. Miah, M. S., Yu, H., Godder, T. K., & Rahman, M. M. (2015). A cluster-based cooperative spectrum sensing in cognitive radio network using eigenvalue detection technique with superposition approach. *International Journal of Distributed Sensor Networks*, 11(7), 207935.

46. Rawat, A. S., Anand, P., Chen, H., & Varshney, P. K. (2010). Collaborative spectrum sensing in the presence of Byzantine attacks in cognitive radio networks. *IEEE Transactions on Signal Processing*, 59(2), 774-786.
47. Ghamry, W. K., & Shukry, S. (2020). Performance evaluation of cooperative eigenvalue spectrum sensing GLRT under different impulsive noise environments in cognitive radio. *Computer Communications*, 160, 567-576.
48. Awin, F., Abdel-Raheem, E., & Tepe, K. (2018). Blind spectrum sensing approaches for interweaved cognitive radio system: A tutorial and short course. *IEEE Communications Surveys & Tutorials*, 21(1), 238-259.
49. Iqbal, Z., Nooshabadi, S., Jadi, K., & Ghasemi, A. (2018, November). Sensor Cooperation and Decision Fusion to Improve Detection in Cognitive Radio Spectrum Sensing. *In 2018 9th IEEE Annual Ubiquitous Computing, Electronics & Mobile Communication Conference (UEMCON)* (pp. 276-281). IEEE.
50. Gul, N., Qureshi, I. M., Omar, A., Elahi, A., & Khan, S. (2017). History based forward and feedback mechanism in cooperative spectrum sensing including malicious users in cognitive radio network. *PloS one*, 12(8), e0183387.
51. Gul, N., Qureshi, I. M., Akbar, S., Kamran, M., & Rasool, I. (2018). One-to-many relationship based kullback leibler divergence against malicious users in cooperative spectrum sensing. *Wireless Communications and Mobile Computing*, 2018.
52. Awasthi, M., Nigam, M. J., & Kumar, V. (2019). Optimal sensing and transmission of energy efficient cognitive radio networks. *Wireless Personal Communications*, 1-12.
53. Kishore, R., Gurugopinath, S., Muhaidat, S., Sofotasios, P. C., Dianati, M., & Al-Dhahir, N. (2020). Energy efficiency analysis of collaborative compressive sensing scheme in cognitive radio networks. *IEEE Transactions on Cognitive Communications and Networking*, 6(3), 1056-1068.
54. Qiao, Y., Jin, Z., Yao, K., & Ma, T. (2018, January). An energy-efficient cooperative spectrum sensing scheme based on ds theory in cognitive radio sensor networks. *In Proceedings of the 12th International Conference on Ubiquitous Information Management and Communication* (pp. 1-6).
55. Ansere, J. A., Han, G., Wang, H., Choi, C., & Wu, C. (2019). A reliable energy efficient dynamic spectrum sensing for cognitive radio IoT networks. *IEEE Internet of Things Journal*, 6(4), 6748-6759.
56. Eappen, G., & Shankar, T. (2020). Hybrid PSO-GSA for energy efficient spectrum sensing in cognitive radio network. *Physical Communication*, 40, 101091.
57. Miah, M. S., Schukat, M., & Barrett, E. (2017, June). Maximization of sum rate in AF-cognitive radio networks using superposition approach and n-out-of-k rule. *In 2017 28th Irish signals and systems conference (ISSC)* (pp. 1-6). IEEE.
58. Jan, S. U., Vu, V. H., & Koo, I. (2018). Throughput maximization using an SVM for multi-class hypothesis-based spectrum sensing in cognitive radio. *Applied Sciences*, 8(3), 421.
59. Vu-Van, H., & Koo, I. (2012). A robust cooperative spectrum sensing based on Kullback-Leibler divergence. *IEICE transactions on communications*, 95(4), 1286-1290.
60. Develi, I. (2020). Spectrum sensing in cognitive radio networks: threshold optimization and analysis. *EURASIP Journal on Wireless Communications and Networking*, 2020(1), 1-19.
61. Tabakovic, Z., & Grgic, M. (2016). Cognitive radio frequency assignment with interference weighting and categorization. *EURASIP Journal on Wireless Communications and Networking*, 2016(1), 1-24.
62. Biswas, S., Dey, S., & Shirazinia, A. (2019). Sum throughput maximization in a cognitive multiple access channel with cooperative spectrum sensing and energy harvesting. *IEEE Transactions on Cognitive Communications and Networking*, 5(2), 382-399.
63. Liu, X., Zheng, K., Chi, K., & Zhu, Y. H. (2020). Cooperative Spectrum Sensing Optimization in Energy-Harvesting Cognitive Radio Networks. *IEEE Transactions on Wireless Communications*, 19(11), 7663-7676.
64. Miah, M. S., Hossain, M. A., Ahmed, K. M., Rahman, M. M., Calhan, A., & Cicioglu, M. (2021). Machine Learning-Based Malicious User Detection in Energy Harvested Cognitive Radio-Internet of Things. *TechRxiv Preprint.*

Figures

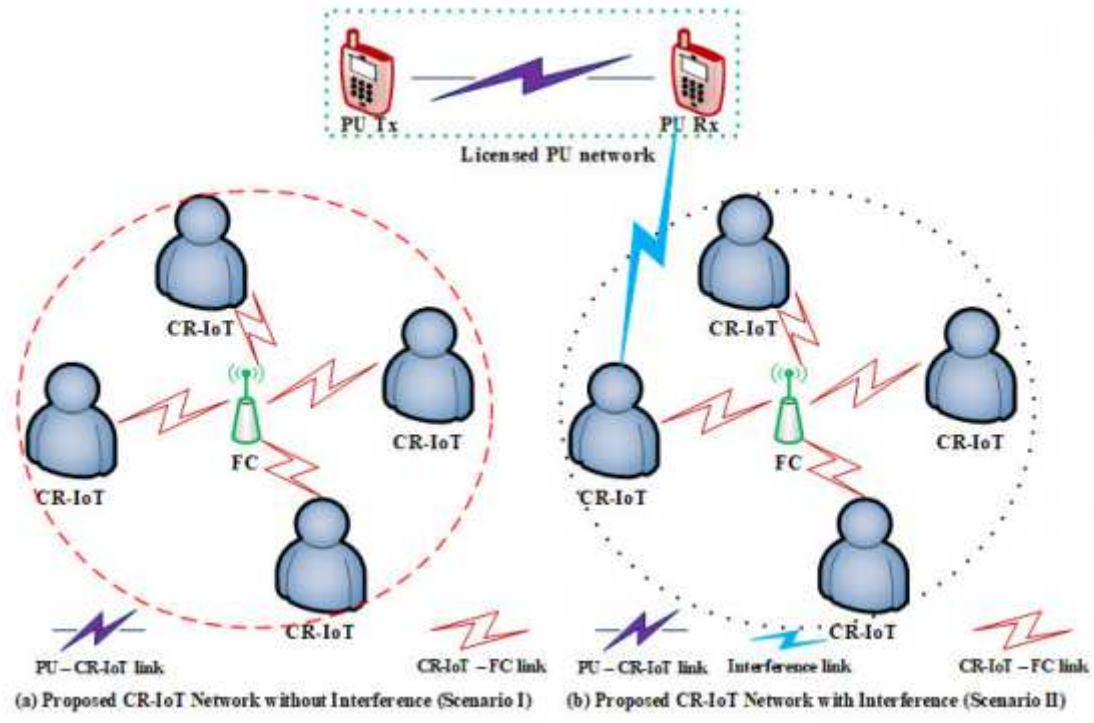

Figure 1

The proposed system model for (a) Scenario I means without interference constraints, and (b) Scenario II means with interference constraints

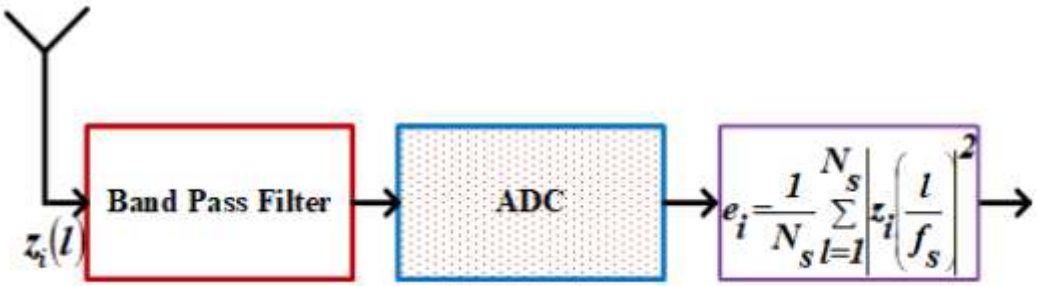

Figure 2

The schematic description of the conventional ED method [17]

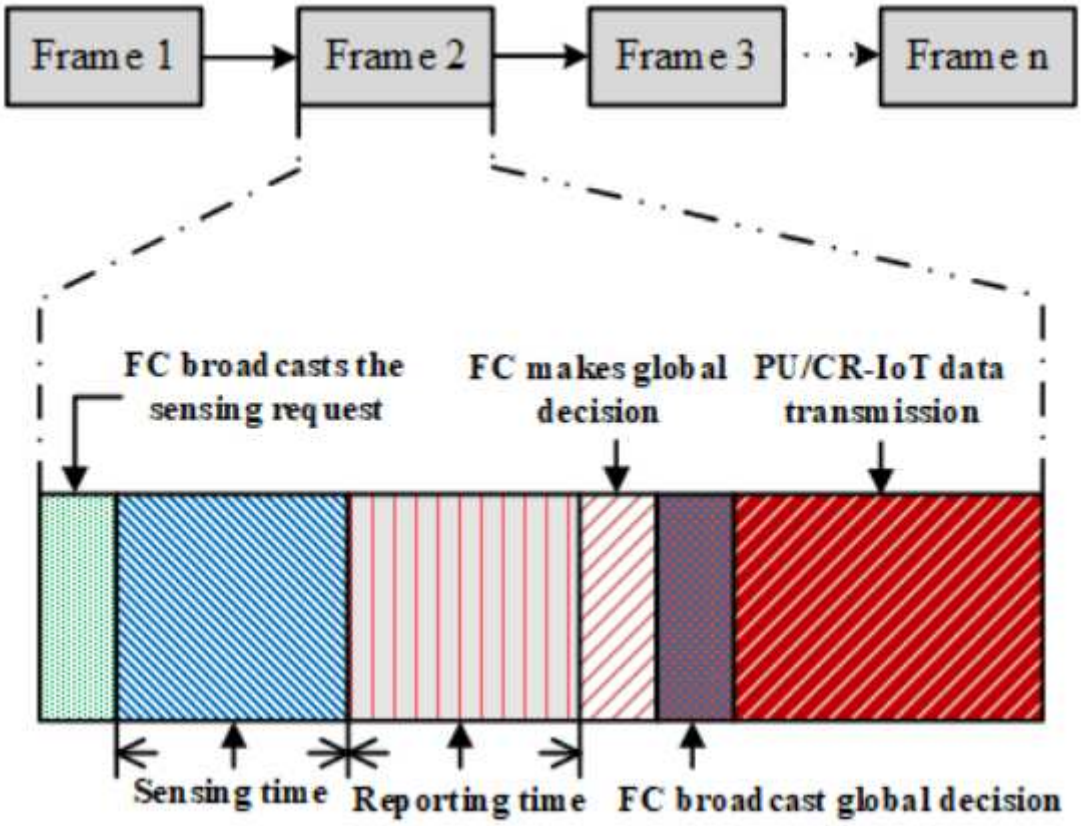

Figure 3

Packet (i.e., each packet consists of the number of frames) format of the typical ED method for scenario I [2, 5, 17]

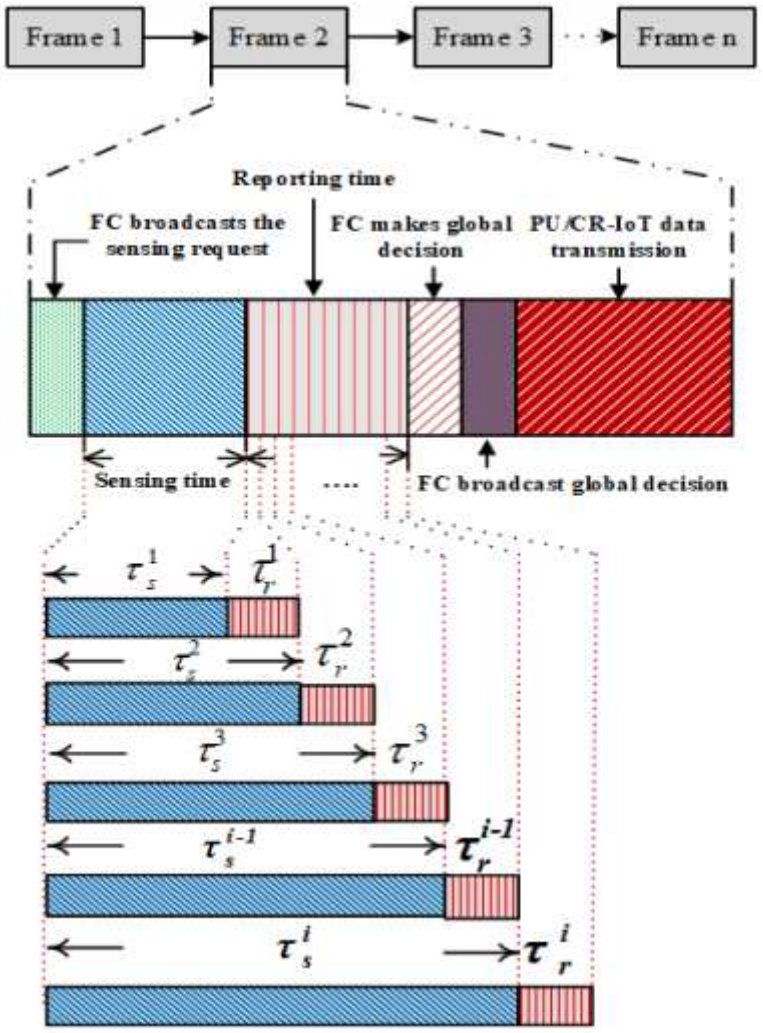

Figure 4

Packet (i.e., each packet consists of the number of frames) format of the proposed ED method for scenario II where the flexible sensing time slot is obtained based on utilized the reporting framework [2]

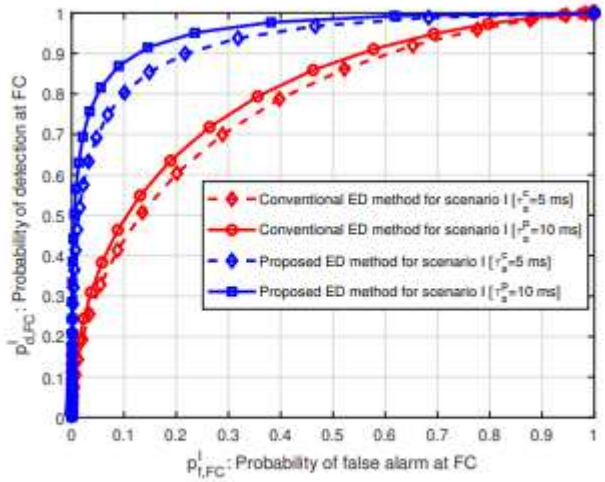

(a) $p^{\mathrm{I}}_{d,FC}$ vs. $p^{\mathrm{I}}_{f,FC}$ for scenario I

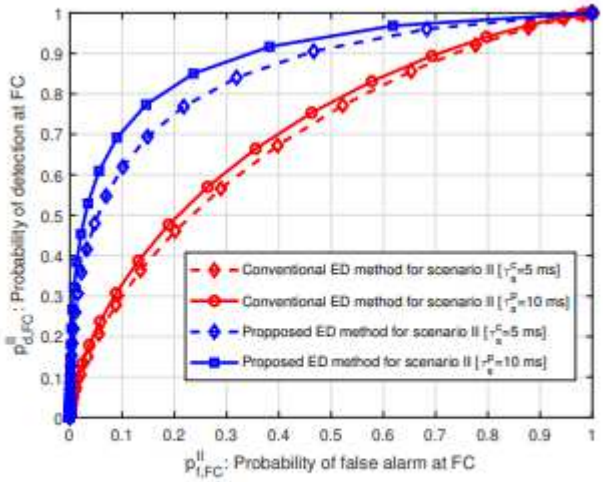

(b) $p^{\mathrm{II}}_{d,FC}$ vs. $p^{\mathrm{II}}_{f,FC}$ for scenario II

Figure 5

The ROC curves for the proposed ED method, and the conventional ED method when both scenario I, and II are considered.

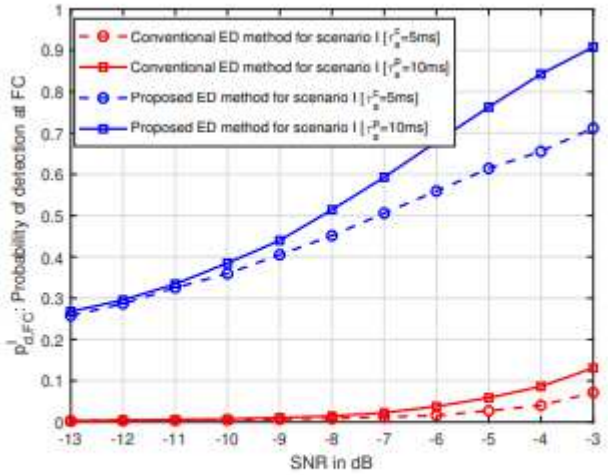

(a) SNR vs. $p^{\mathbb{I}}_{d,FC}$ for scenario $\mathbb{I}$

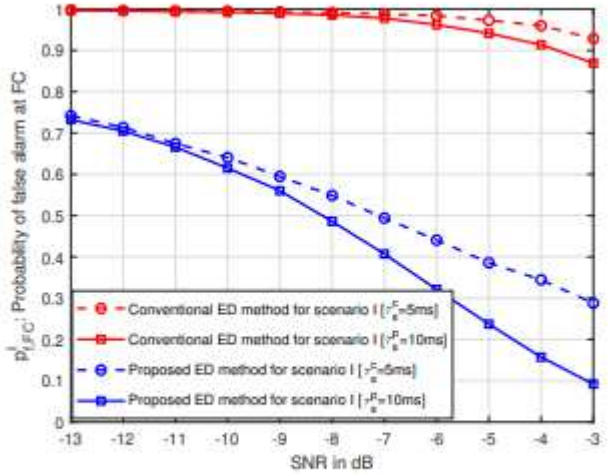

(b) SNR vs. $p^{\mathbb{I}}_{f,FC}$ for scenario $\mathbb{I}$

Figure 6

SNR vs. the detection probability, and the probability of false alarm at FC when scenario I is only considered.

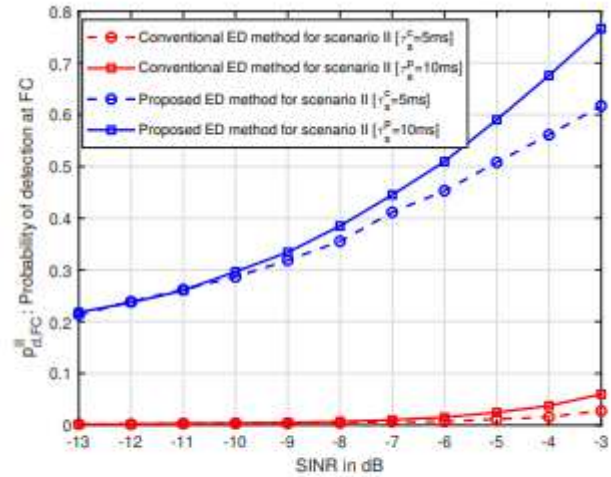

(a) SINR vs the detection probability for scenario $\mathbb{III}$

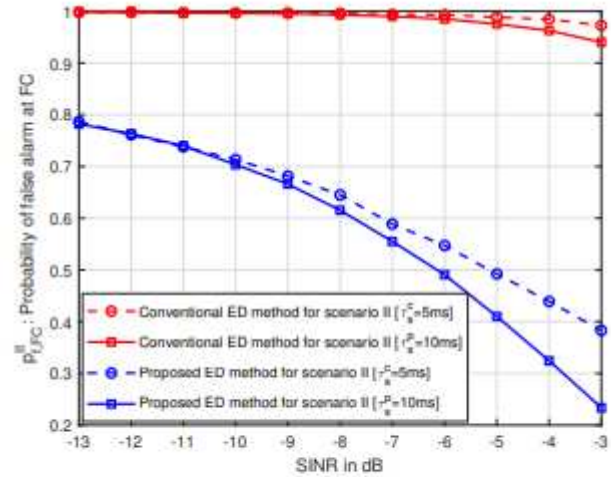

(b) SINR vs the probability of false alarm for scenario $\mathbb{III}$

Figure 7

SINR vs. the detection probability, and the probability of false alarm at FC when scenario II is only considered.

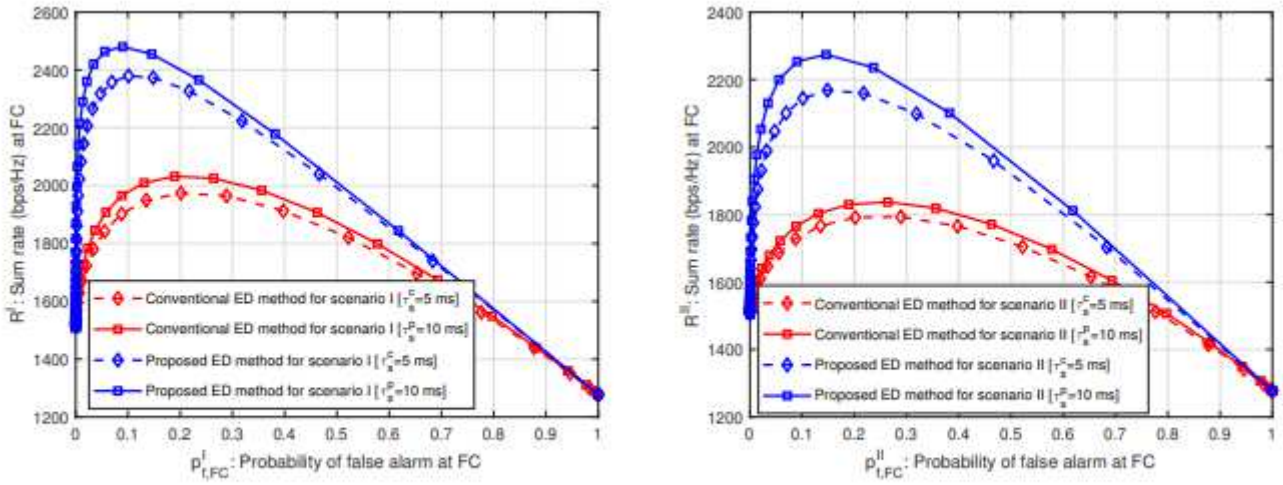

(a) $\mathbb{R}^{\mathbb{I}}$ vs. $p^{\mathbb{I}}_{f,FC}$ for scenario $\mathbb{I}$ (b) $\mathbb{R}^{\mathbb{II}}$ vs. $p^{\mathbb{III}}_{f,FC}$ for scenario $\mathbb{III}$

Figure 8

Sum rate curves at FC of the conventional ED method, and the proposed ED method when scenario I, scenario II, and α = 0.7 are considered.

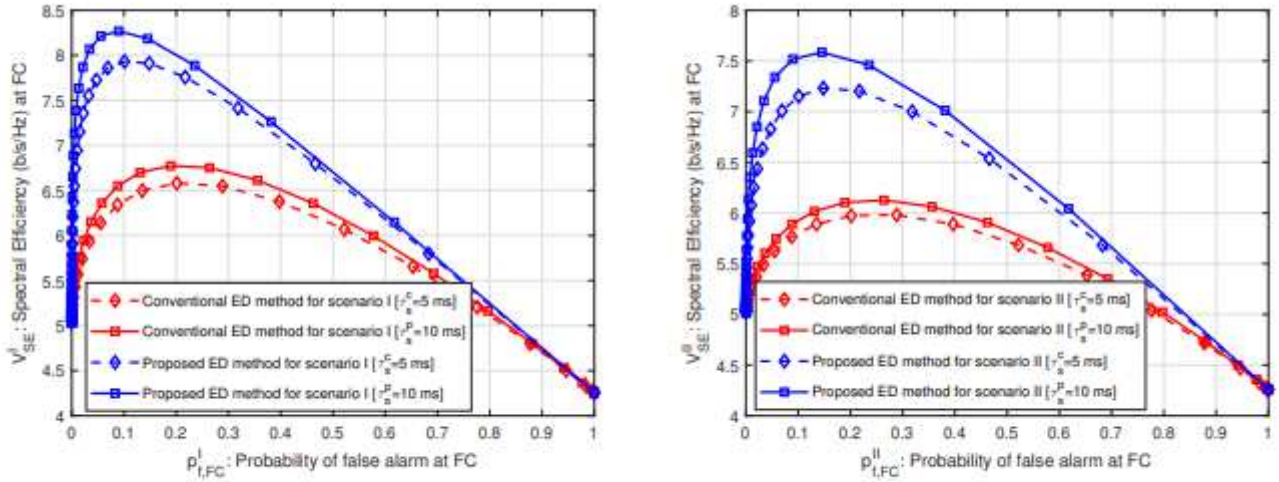

(a) SE vs. $p^{\mathbb{I}}_{f,FC}$ for scenario $\mathbb{I}$ (b) SE vs. $p^{\mathbb{III}}_{f,FC}$ for scenario $\mathbb{III}$

Figure 9

Spectral efficiency curves at FC of the conventional ED method and the proposed ED method when both scenario I and scenario II are considered.

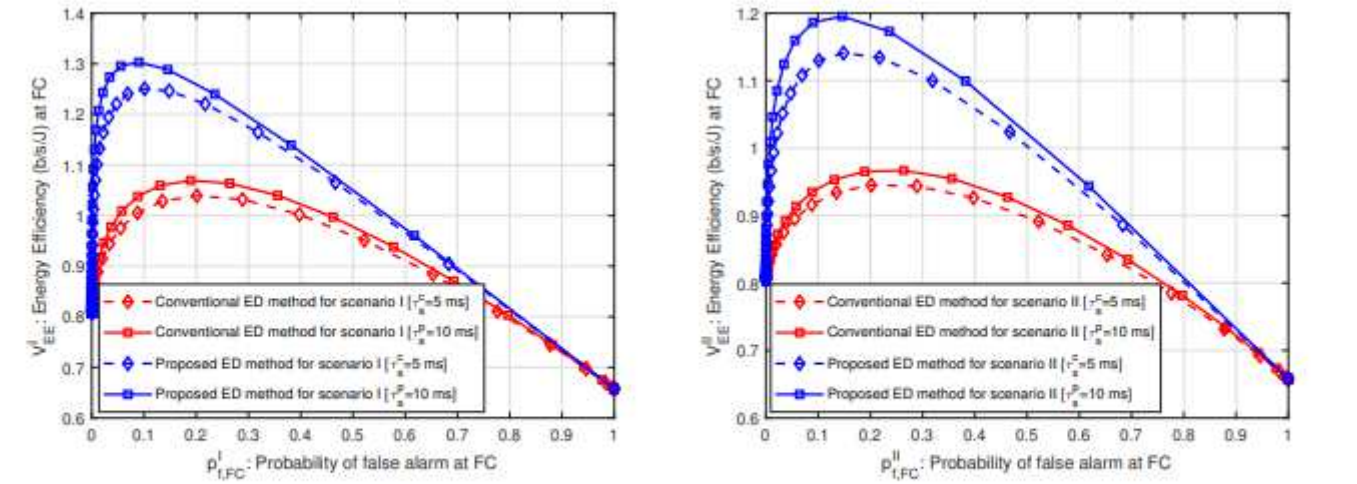

(a) Energy efficiency vs. $p_{f,FC}^{\mathbb{I}}$ under scenario $\mathbb{I}$ (b) Energy efficiency vs. $p_{f,FC}^{\mathbb{III}}$ under scenario $\mathbb{III}$

Figure 10

Energy efficiency curves vs. the probability of false alarm at FC for the conventional ED method, and the proposed ED method when scenario I and scenario II are considered.

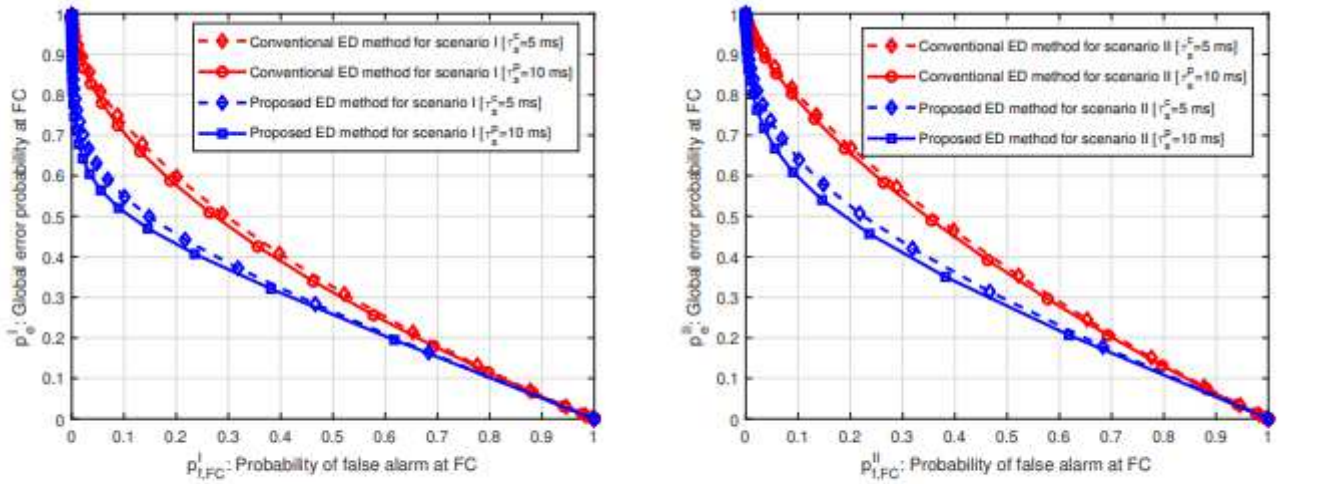

(a) Global error probability curves versus $p_{f,FC}^{\mathbb{I}}$ at FC for scenario $\mathbb{I}$ (b) Global error probability curves versus $p_{f,FC}^{\mathbb{III}}$ at FC for scenario $\mathbb{III}$

Figure 11

Global error probability curves at FC of the conventional ED method and the proposed ED method when scenario I and scenario II are considered.